



Contents lists available at ScienceDirect

Ore Geology Reviews

journal homepage: www.elsevier.com/locate/oregeo

Lithostratigraphic and structural reconstruction of the Zn-Pb-Cu-Ag-Au Lemarchant volcanogenic massive sulphide (VMS) deposit, Tally Pond group, central Newfoundland, Canada

Jonathan Cloutier^{a,*}, Stephen J. Piercey^a, Stefanie Lode^a, Michael Vande Guchte^b, David A. Copeland^b^a Department of Earth Sciences, Memorial University of Newfoundland, 300 Prince Philip Drive, St. John's, Newfoundland and Labrador A1B 3X5, Canada^b Canadian Zinc Corporation, Suite 1710, 650 West Georgia Street, PO Box 11644, Vancouver, British Columbia V6B 4N9, Canada

ARTICLE INFO

Article history:

Received 2 October 2016

Received in revised form 6 January 2017

Accepted 11 January 2017

Available online 12 January 2017

Keywords:

Precious metal enriched VMS deposits

Lemarchant deposit

Tally Pond

Stratigraphic reconstruction

Structural reconstruction

Appalachian tectonic evolution

ABSTRACT

The Lemarchant volcanogenic massive sulphide (VMS) deposit (1.24 Mt grading at 0.58% Cu, 5.38% Zn, 1.19% Pb, 1.01 g/t Au, and 59.17 g/t Ag) is a bimodal-felsic VMS deposit hosted within the Late Cambrian (~513–509 Ma) Tally Pond group of the Exploit Subzone in central Newfoundland, Canada. The deposit is hosted by andesitic volcanoclastic and volcanic rocks with subordinate dacite flows. The mineralisation is hosted by the dacites and is overlain by pillowed and massive basalts.

Four structural breaks offset the local stratigraphic sequences including: 1) the LJ syn-volcanic shear zone; 2) the KJ syn-volcanic shear zone; 3) the Lemarchant thrust; and 4) the Bam normal fault. Deformation of the Lemarchant likely occurred during the Penobscot orogeny (486–478 Ma). Early deformation is marked with the local deformation of the LJ and KJ syn-volcanic shear zones during NW-SE compression which coincided with the development of the Lemarchant thrust. A late (<465 Ma) east trending normal fault, the Bam fault, affected the central portion of the Lemarchant area and down-faulted the southern portion of the study area relative to the northern portion.

Immobile element systematics of all the sequences from the Lemarchant deposit are tholeiitic with transitional Zr/Y ratios (1.9–6.6), La_n/Sm_n ratios <1 (normalised to upper crust), and have primitive mantle extended rare earth elements profiles with slight light rare earth element (LREE)-enriched patterns with flat heavy REE (HREE), and weak to strong negative Nb, Zr, and Ti anomalies. Together, these geochemical features, coupled with an F11a signature, and existing mineralogical and Nd-Pb isotope data, are consistent with the rocks at the Lemarchant deposit having formed within a shallow (<1500 m) arc or migrating cross-arc seamount chain located within a young peri-continental rifted arc along the margin of Ganderia, within the Iapetus Ocean. The estimated shallow water emplacement of the deposit likely allowed boiling near or at the rock-sea water interface, ultimately resulting in precious metal enrichment of the Lemarchant deposit. It is suggested that cross-arcs within rifted arc environments may represent favourable exploration targets for precious metal-enriched VMS deposits.

© 2017 Elsevier B.V. All rights reserved.

1. Introduction

The Lemarchant deposit is a type example of an Appalachian precious metal-bearing bimodal-felsic volcanogenic massive sulphide (VMS) deposit (Fig. 1). Globally, bimodal-felsic (i.e., Kuroko-type) VMS deposits are commonly Zn-Pb-Cu-rich, stratabound to stratiform, syngenetic deposits that form on, or near,

the seafloor by precipitation from hydrothermal fluids (e.g., Large, 1977; Franklin et al., 1981, 2005; Lydon, 1984, 1988; Hannington, 2014). They are commonly capped by massive barite and hydrothermal exhalative mudstone.

Bimodal-felsic hosted deposits form near eruptive centres and are commonly hosted within autoclastic rhyolitic volcanoclastic rocks to massive rhyolite flows (e.g., Ohmoto, 1996; Lizasa et al., 1999; McNicoll et al., 2010; Piercey et al., 2014). Bimodal-felsic deposits, like all VMS deposits, form within extensional geodynamic regimes, commonly in arc rifts and back-arc basins (e.g., Swinden, 1991; Piercey, 2010, 2011; Hannington,

* Corresponding author at: Department of Earth and Environmental Sciences, University of St Andrews, North Street, St Andrews KY16 9AL, UK.

E-mail address: jc301@st-andrews.ac.uk (J. Cloutier).

2014). In ancient environments, the extensional stage of tectonic activity is frequently followed by uplift, basin inversion, compressional deformation, and metamorphism of the sequence hosting the massive sulphide deposits often related to post-VMS formation accretionary tectonics (e.g., McClay, 1995; Nelson, 1997). Consequently, lithostratigraphic and structural reconstructions of VMS deposits in ancient accretionary orogens are critical to understand the genesis of ancient VMS deposits, as well as their exploration.

The Lemarchant deposit provides the opportunity to study deformed VMS mineralisation systems in an accretionary orogenic setting. The level of stratigraphic preservation and the predominantly brittle deformation at Lemarchant allows for its reconstruction in 3D, unlike many other volcanic belts where high intensity of deformation obscures original stratigraphy (i.e., more structurally complex and ductile in nature) or where outcrop distribution and diamond drilling density are insufficient to undertake the reconstruction. The aim of this study is to document the stratigraphy and major structures affecting the Lemarchant VMS deposit to understand the subsurface distribution of the structural features and geologic units, including the mineralisation, using a three-dimensional framework. In addition, this study presents new geochemical data obtained at the Lemarchant deposit and assess the immobile element geochemical signatures and the tectonic evolution of the Lemarchant deposit and Tally Pond group. This reconstruction resolves the primary origin for mineralised zones, provides new information on the tectonic evolution of the Tally Pond group and the Appalachian mountain belt, and generates new exploration concepts for VMS deposits. The results herein have implications not only for Appalachian VMS environments, but for any deformed and imbricated VMS belts globally.

2. Geology

2.1. Regional geology

The Cambrian (513–509 Ma) Lemarchant VMS deposit is located within the Dunnage Zone of the Appalachian mountain belt of central Newfoundland, Canada (Fig. 1; Copeland, 2008). The Dunnage Zone is bounded by the Humber Zone to the west and the Gander Zone to the east (Williams, 1979; Williams et al., 1988; Hibbard et al., 2004), and represents the deformed vestiges of arcs, back-arcs and ophiolite complexes assembled during the closure of the Cambrian to Ordovician Iapetus Ocean (Fig. 1; Williams, 1979; Williams et al., 1988; Swinden et al., 1989; Swinden, 1991; Kean et al., 1995; van Staal and Colman-Sadd, 1997; Evans and Kean, 2002; Rogers and van Staal, 2002; Rogers et al., 2006; van Staal, 2007; Zagorevski et al., 2010). The Dunnage Zone is divided into the Notre Dame Subzone, which formed near the Laurentian equatorial margin, and the Exploits Subzone, which formed on the edge of Gondwana and related microcontinents at mid- to high-southerly latitudes (e.g., Williams et al., 1988; Cocks and Torsvik, 2002; Zagorevski et al., 2006; van Staal, 2007). The suture zone between these two subzones is marked by the Red Indian Line, a 2–3 km wide mylonitic shear zone gently dipping towards the northwest (Fig. 1; e.g. O'Brien et al., 1991; Cocks and Torsvik, 2002; Zagorevski et al., 2006; van Staal, 2007). The Exploits Subzone is divided into four geotectonic domains (Figs. 1 and 2), which are: 1) the Neoproterozoic arc and back-arc remnants derived from Ganderia; 2) the 513–488 Ma arc and back-arc volcanic sequences of the Penobscot Arc, which hosts the Lemarchant deposit and numerous other VMS deposits (Fig. 2; e.g., Duck Pond and the Boundary deposits); 3) the 473–455 Ma arc and back-arc volcanoclastic and sedimentary sequences of the Popelogan-Victoria Arc,

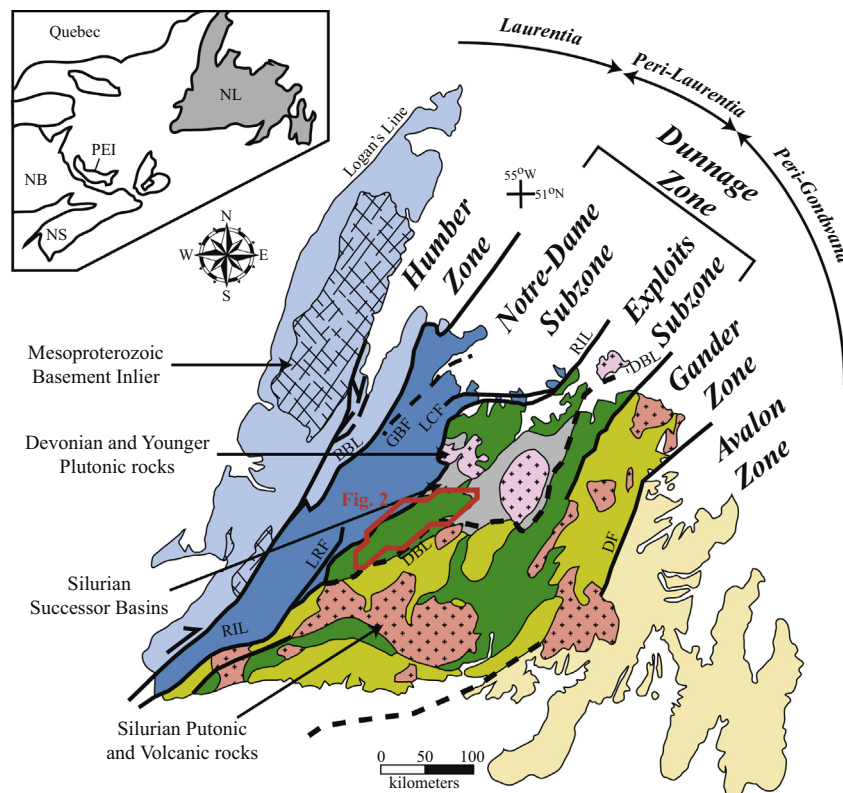


Fig. 1. Simplified geological map of the Newfoundland with tectonostratigraphic zones (modified from van Staal 2007, and van Staal and Barr 2012). Abbreviations are as follow: BBL: Baie Verte Brompton Line, DBL: Dog Bay Line, DF: Dover Fault, GBF: Green Bay fault, LCF: Lobster Cove fault, LRF: Lloyds River fault, and RIL: Red Indian Line.

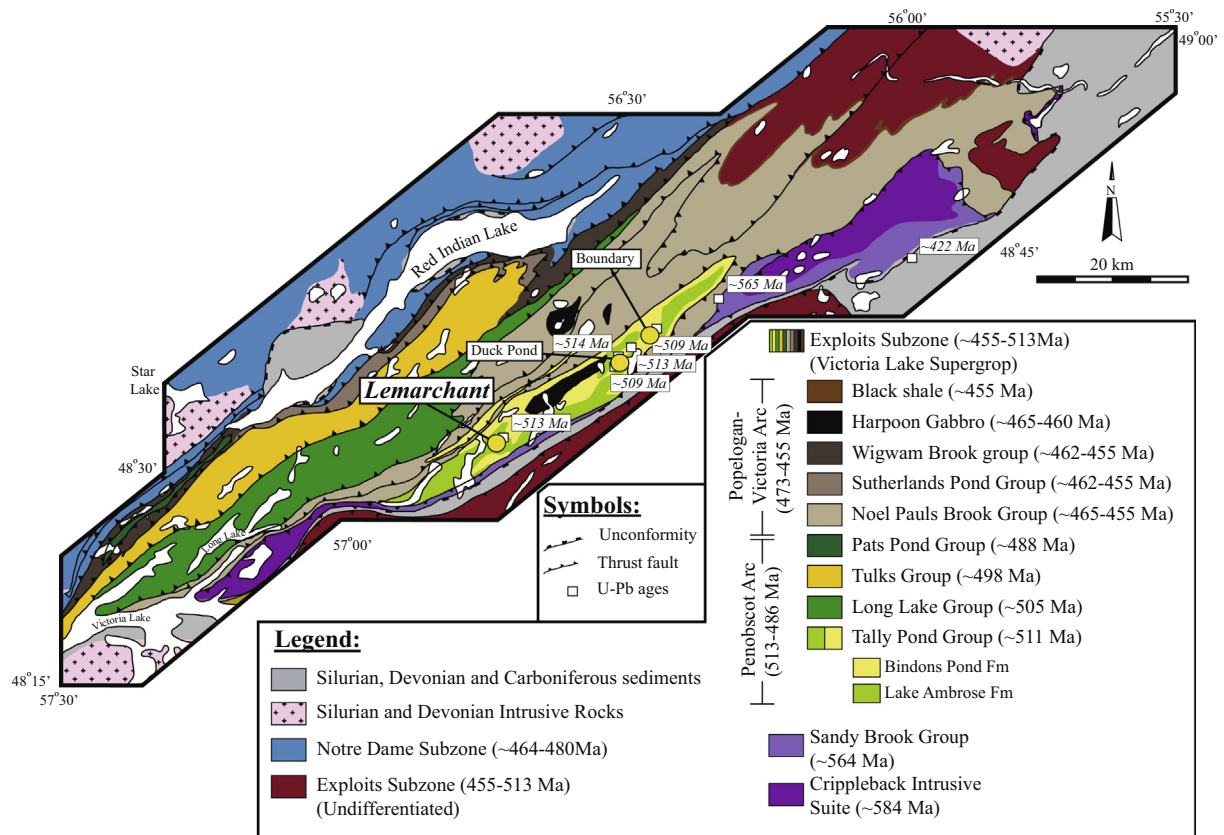


Fig. 2. Geologic setting of the Victoria Lake supergroup, as well as the VMS deposit hosted within the Tally Pond group. Diagram modified from McNicoll et al. (2010) and Piercey et al. (2014).

which was built in part on the older Penobscot Arc; and 4) younger marine sedimentary rocks covering the Popelogan-Victoria Arc sequence (Dunning and Krogh, 1985; Dunning et al., 1987, 1991; Evans et al., 1990; Squires et al., 1991, 2001; Colman-Sadd et al., 1992; O'Brien et al., 1997; MacLachlan and Dunning 1998a,b; MacLachlan et al., 2001; Evans and Kean, 2002; Squires and Moore, 2004; Rogers et al., 2006; Zagorevski et al., 2007b; Zagorevski et al., 2010; McNicoll et al., 2008, 2010; van Staal and Barr, 2012; Piercey et al., 2014). These arcs and related back-arcs sequences were accreted onto the passive margin of Ganderia during the Penobscot Orogeny (486–478 Ma; Colman-Sadd et al., 1992; van Staal, 1994; Johnson et al., 2009; Zagorevski et al., 2010), and to Laurentia during phase 3 of the Taconic Orogeny (~461 to ~450 Ma; Zagorevski et al., 2010; van Staal, 2007; van Staal and Barr, 2012).

The Lemarchant deposit is occurs within the Victoria Lake supergroup, which includes elements of both the Penobscot and Popelogan-Victoria arcs (Fig. 2). Elements of the Penobscot Arc include: the 513–509 Ma bimodal volcanic rocks of the Tally Pond group, which hosts the Lemarchant deposit (Dunning et al., 1991; Rogers et al., 2006; McNicoll et al., 2008); the 514–506 Ma bimodal volcanic rocks of the Long Lake group (Zagorevski et al., 2007a; Hinchey and McNicoll 2016); the 496.5 ± 1 Ma dominantly felsic with minor mafic volcanic rocks of the Tulks group (G.R. Dunning, personal communication, 2008); and the 491–488 Ma bimodal volcanic rocks of the Pats Pond group (Zagorevski et al., 2007a; Hinchey and McNicoll, 2009). Elements of the Popelogan-Victoria Arc comprise the >465 Ma to >455 Ma dominantly sedimentary with minor felsic volcanic rocks of the Noel Paul's Brook Group (Dunning et al., 1987; Zagorevski et al., 2008), the 462–457 Ma sedimentary rocks of the Sutherlands Pond group (Dunning et al., 1987; Zagorevski et al., 2008) and the ~453 Ma sedimentary, felsic

volcaniclastic and subordinate mafic volcanic rocks of the Wigwam Brook group (Zagorevski et al., 2007a).

The Tally Pond group has been informally subdivided into two units that include the predominantly mafic Lake Ambrose formation and the predominantly felsic Bindons Pond formations (Rogers and van Staal, 2002; Rogers et al., 2006). The Lake Ambrose formation consists of vesicular to amygdaloidal, dark green to grey, massive to locally pillowed tholeiitic basalt flows and subordinate tuff, pillow breccia, volcanic breccia and andesitic flows. Geochemically, rocks from the Lake Ambrose formation are predominantly arc tholeiites with $\epsilon\text{Nd}_t > 0$ (Rogers et al., 2006). Felsic volcanic rocks of the Bindons Pond formation comprise massive to flow-banded aphyric dacite and rhyolite, quartz- and/or feldspar-phyric rhyolite, volcaniclastic, epiclastic, and crystal tuff, volcanic breccia and subvolcanic quartz porphyry. Geochemically, they have calc-alkalic to transitional signatures with ϵNd_t ranging from +1.77 to -2.64 indicative of both juvenile and evolved components in their genesis (Rogers et al., 2006). Regionally, the rocks of the Lake Ambrose formation are found stratigraphically below the Bindons Pond formation (Kean and Evans, 1986; Evans and Kean, 2002; Rogers and van Staal, 2002; Rogers et al., 2006) but at Lemarchant, they are found stratigraphically overlying the Bindons Pond formation (Copeland, 2008).

2.2. Geology of the Lemarchant deposit

The Lemarchant deposit consists of two mineralised zones: the Main Zone and the Northwest Zone (Fig. 3). The Main Zone contains an indicated resource of 1.24 million tonnes grading at 5.38% Zn, 0.58% Cu, 1.19% Pb, 1.01 g/t Au and 59.17 g/t Ag and an inferred resource of 1.34 million tonnes grading 3.70% Zn, 0.41% Cu, 0.86% Pb, 1.00 g/t Au and 50.41 g/t Ag (NI43-101;

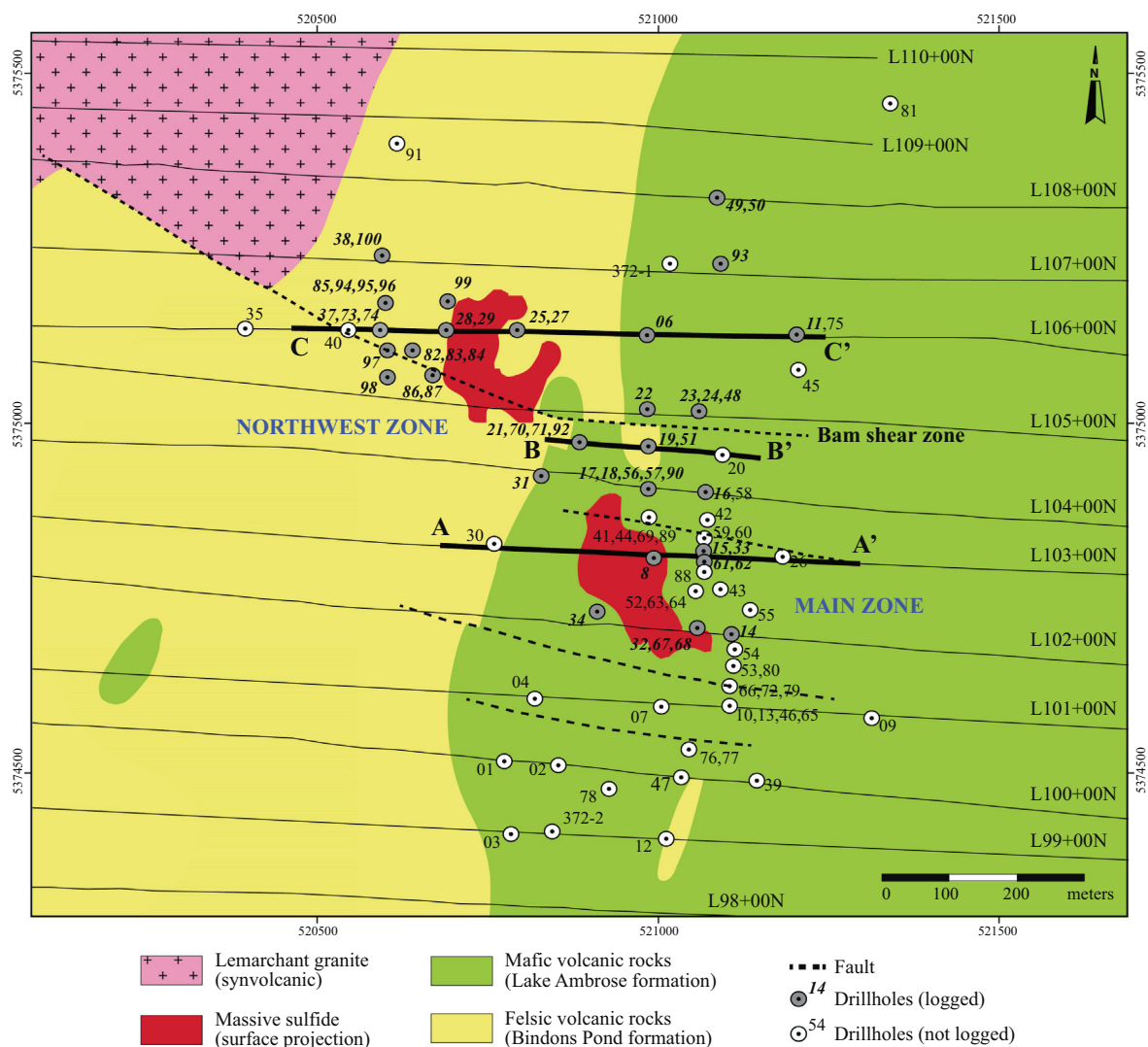


Fig. 3. Geological map of the Lemarchant area and projected surface location of the Main and Northwest mineralised zones. Also shown are the cross-section lines (A-A', B-B', and C-C') described in Fig. 5. Map modified from Fraser et al. (2012).

Fraser et al., 2012). At present, there is no NI-43-101 compliant resource for the Northwest Zone. Both zones are hosted by massive felsic flows of the Bindons Pond formation and are separated by a structurally complex corridor. They are interpreted to represent two parts of a single dismembered sulphide lens that have been displaced by the Lemarchant fault (Fraser et al., 2012). However, given the structural complexity of the corridor, it is possible that these two mineralised zones represent different mineralised lenses that were superimposed during post-VMS formation deformation.

The Main Zone ranges in thickness from 1.7 to 30.4 m, strikes south-southwest, dips shallowly towards the northwest, and is occurs near or at the contact with the conformable mafic volcanic rocks of the Lake Ambrose formation (Copeland, 2008; Fraser et al., 2012; Gill, 2015). The Northwest Zone ranges in thickness from 1.8 to 29.8 m, strikes northwest, dips steeply ($\sim 60^\circ$) towards the northeast (Fraser et al., 2012).

The mineralisation in both zones consists of <30 m thick lenses of massive, semi-massive, and stringers of sphalerite, chalcopyrite, galena, pyrite, pyrrhotite, and barite that precipitated in three stages (Gill et al., 2013, 2015, in press; Gill and Piercey, 2014). Stage 1 is characterised by precipitation of low-Fe sphalerite and pyrite whereas Stage 2 is marked by precipitation of sulphosalts

(i.e., tetrahedrite-tennantite), bornite, stromeryite, electrum, bladed barite, Ca-Fe-Mg-Mn-carbonate, and enrichments in epithermal suite elements (i.e., Au, As, Bi, Co, Cr, In, Mo, Ni, Sb, Se, Te), which are atypical of VMS deposits (Gill et al., 2013, 2015, in press; Gill and Piercey, 2014). Both stages are interpreted to have formed at relatively low temperature (150–250 °C) in a shallow water environment (<1500 m below sea level (mbsl)) wherein intermitted boiling principally occurred during Stage 2 and produced the Ag and Au enrichment observed at the Lemarchant deposit (Gill et al., 2013, 2015, in press; Gill and Piercey, 2014). Stage 3 consists of a late overprint of stages 1 and 2 assemblages by chalcopyrite and pyrite, and the creation of a stringer zone below the stratiform zone of the Lemarchant deposit. It is interpreted as a return to more “typical” VMS conditions, and correlate with a marked increase in the temperature of the hydrothermal fluids (>300 °C). Stage 3 is also associated with a deepening of the basin to >1500 mbsl due to the absence of epithermal suite elements and the lack of boiling evidences (Gill et al., 2013, 2015, in press; Gill and Piercey, 2014).

A thin layer of discontinuous exhalative mudstone (<1–20 m) caps the massive sulphide lenses and extends to four kilometres from the deposit (Copeland, 2008; Fraser et al., 2012; Lode et al., 2015, 2016). Hydrothermal alteration associated with the

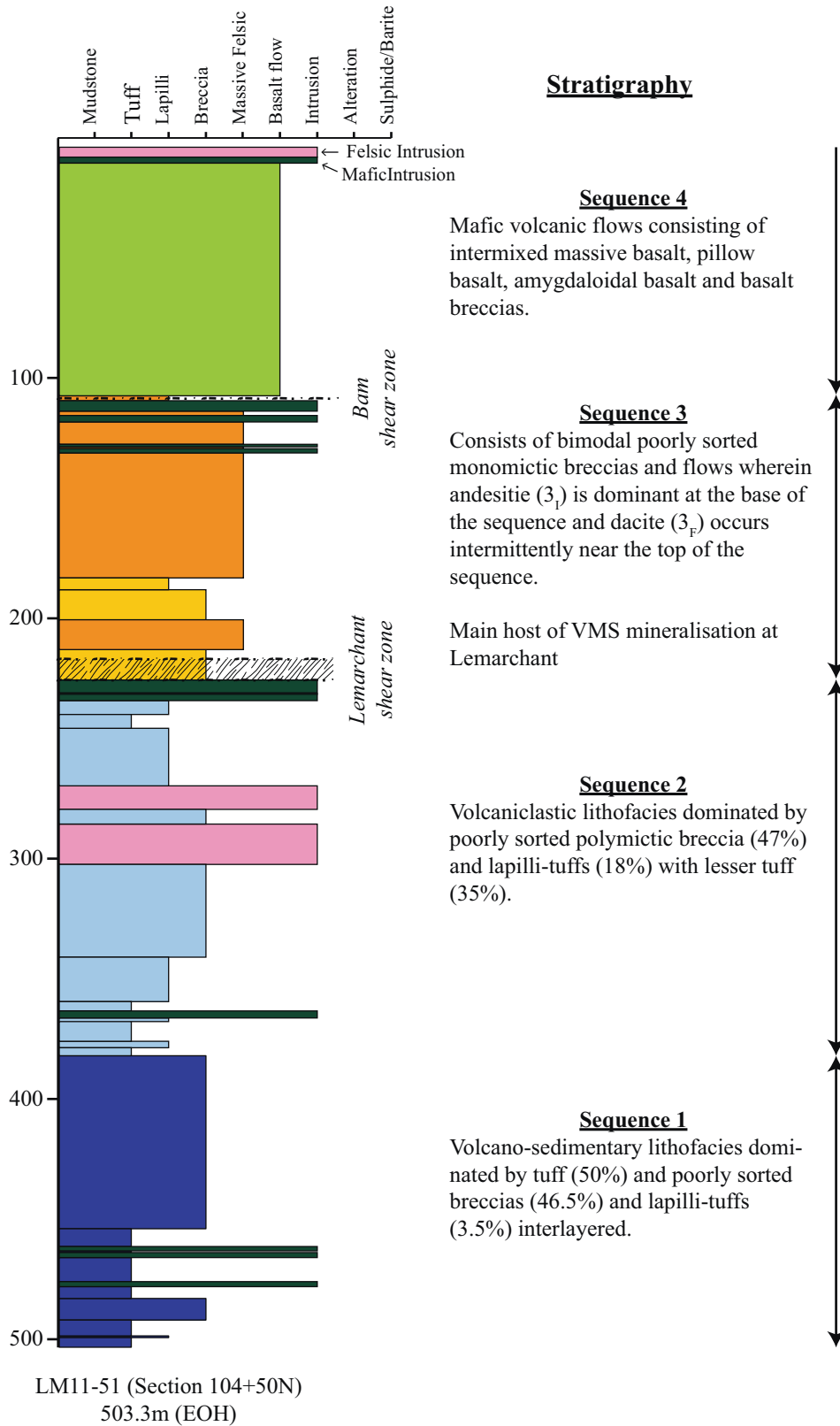


Fig. 4. Lithostratigraphic sequence from drill core LM11-51 (section 104+50N) representative of the Lemarchant area. Also shown is the summary of the key features of each sequence.

mineralised zones is characterised by intense and localized Ba-enrichment, quartz, sericite and chlorite hydrothermal alteration (Fraser et al., 2012). At present, the alteration associated with the Lemarchant deposit has been outlined over 4 km in strike and

is open to the north and south (Copeland, 2008; Fraser et al., 2012). Post-mineralisation, possibly syn-mafic volcanic, mafic and felsic dikes intrude the felsic and mafic volcaniclastic and volcanic rocks of the Tally Pond group.

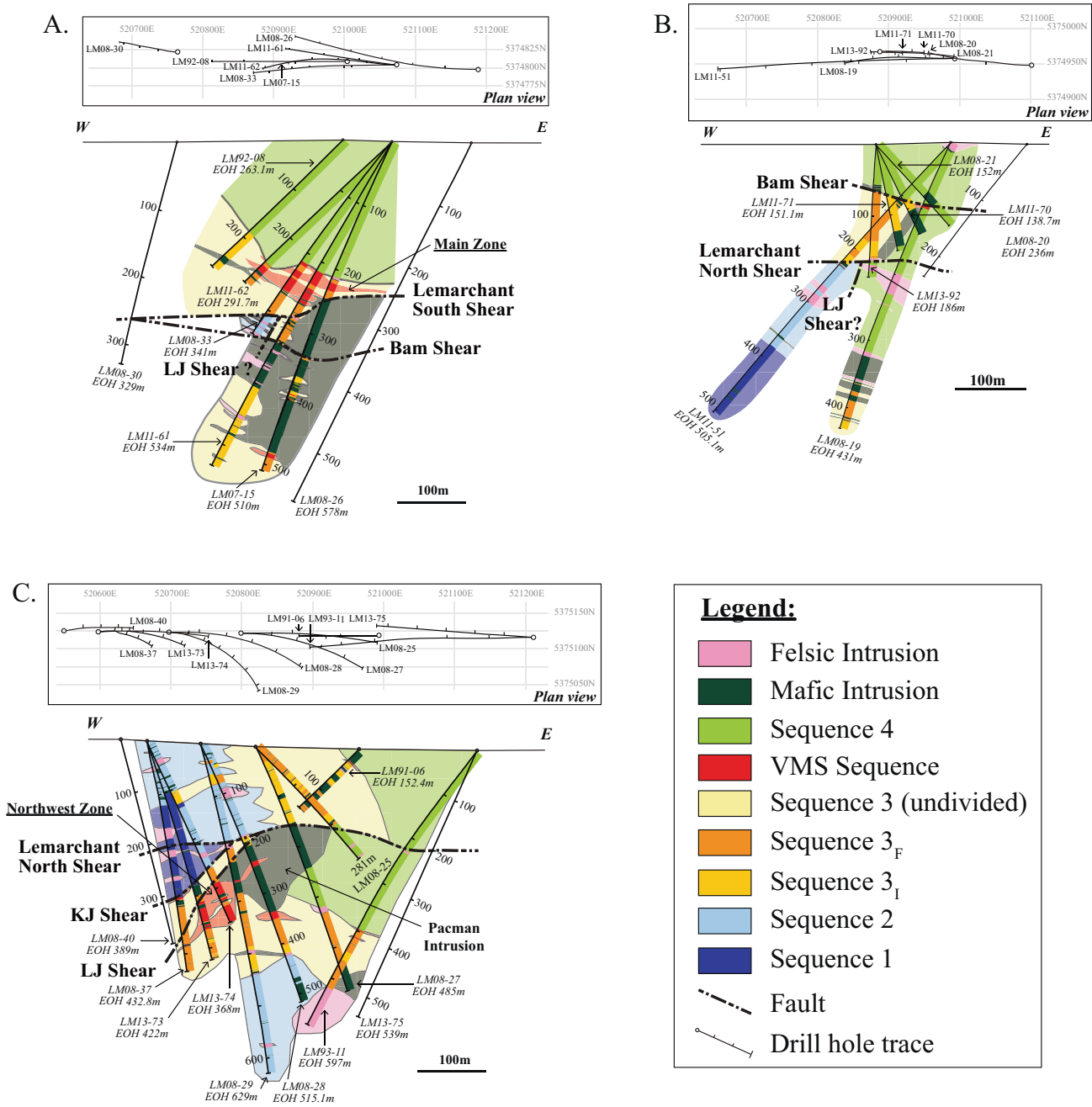


Fig. 5. Cross-section along (A) the southern portion (section 103+00N; Main Zone), (B) the central portion (section 104+50N, and (C) the northern portion (106+00N; Northern Zone) of the Lemarchant area.

Post-mineralisation deformation of the deposit occurred along the Lemarchant thrust fault (Copeland, 2008; Fraser et al., 2012). Late east-southeast trending and southerly dipping normal faults also displaced the Main Zone between sections 104+00N and 106+00N (Fig. 3).

3. Stratigraphic sequences

A total of 53 diamond drill cores from 10 sections across the Lemarchant area were logged to identify and map the main structures and lithostratigraphic units present in area. The volcanoclastic

lithofacies described herein are classified using the classification of Fisher (1966), which has been updated by White and Houghton (2006). These classifications are non-genetic and based entirely on clast size and abundance, with no implications for the nature or mechanism of emplacement. Lithogeochemistry is discussed in detail in the following section; however, the rock nomenclature based on immobile trace elements is presented herein for chemostratigraphic purposes. Four volcano-sedimentary sequences, one mineralised sequence, and several intrusive phases are recognised at the Lemarchant deposit. The lithological sequences from a representative drill core (LM11-51 from section 104+50N), three cross-sections from section lines 103+00N, 104

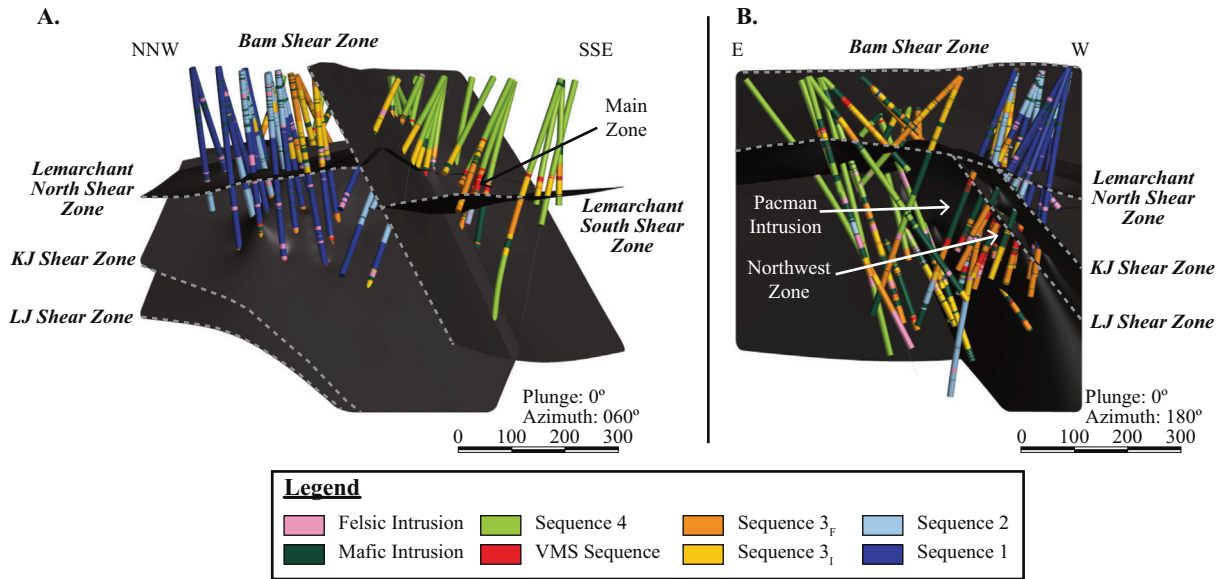


Fig. 6. Three-dimension representation of the lithostratigraphic sequences logged during this study. Also shown are the structural elements present in the Lemarchant area and the location of the Main and Northwest mineralised zones. (A) Looking ENE (060°) and (B) looking south (180°).

+50N, and 160+00N, and a three-dimensional model of the distribution of the subsurface lithology are presented in Figs. 4–6 respectively. Overall, the lithostratigraphic sequences of the Lemarchant deposit reflect an evolution from a distal (sequences 1 and 2) volcanoclastic dominated environment of formation to a proximal (sequence 3) volcanic dominated depositional environment.

3.1. Sequence 1

Sequence 1 is found at the base of the stratigraphy at the Lemarchant area and chemically falls within the basalt/andesite field of Pearce (1996) (Fig. 7a). The sequence consists of volcanosedimentary lithofacies dominated by tuff (50%) and poorly sorted breccias (46.5%) and lapilli-tuffs (3.5%). The tuff is andesitic in composition, is grey to dark blue in colour and consists of >90% matrix with rare small (2–20 mm) monolithic clasts and flattened carbonate filled cavities (Figs. 7a, 8c). Minor <30 mm circular to elliptical, red to orange staining of the rock is also characteristic of this lithofacies.

The lapilli-tuff and breccia are grey to dark blue-green in colour and contain >50% angular to subrounded andesitic clasts. Rare subrounded to rounded basaltic clasts and polyolithic breccia clasts consisting of red chert, felsic, intermediate and mafic fragments occurs locally (Fig. 8ab), suggesting a multi-source provenance. Characteristic interstitial dark chlorite aggregates are interstitial to the clasts to the volcanoclastic rocks matrix (Fig. 8a), and likely to reflect seawater alteration of volcanic glass shards shortly after their formation. When clast-supported, the chlorite aggregates within the breccias and lapilli-tuffs may account for up to 100% of the inter-clast matrix.

Sequence 1 is constrained to the northwest and west portion of the Lemarchant area and is found in the hanging wall of the KJ and the Lemarchant shear zones, and in the footwall (north side) of the Bam fault (Figs. 5 and 6).

3.2. Sequence 2

Sequence 2 falls within the basalt/andesite field of Pearce (1996) and consists of volcanoclastic lithofacies dominated by

poorly sorted polymictic breccia (47%) and lapilli-tuffs (18%) with lesser tuff (35%) (Fig. 8a). The lapilli-tuffs and breccias are pale grey to dark grey in colour and generally contain >50% clasts. The clasts are angular to subrounded and dominated by andesitic clasts with subordinate subrounded to rounded smaller mafic and chert clasts (Figs. 7a, 8d). Unlike rocks of sequence 1, polymictic clasts and interstitial aggregate of dark chlorite are absent in the matrix of the volcanoclastic rocks of sequence 2.

The tuff of sequence 2 is macroscopically and chemically indistinguishable from those of sequence 1 (Fig. 8e), except that the tuff intervals from sequence 2 are generally restricted to a few meters compared to the 10s to 100s of meters of the tuffs of sequence 1.

Sequence 2 conformably overlies sequence 1 and is constrained to the northwest portion of the Lemarchant area. Like sequence 1, it is found in the hanging wall of the KJ and the Lemarchant shear zones, and in the footwall (north side) of the Lemarchant shear zone and Bam fault (see section 5; Figs. 5 and 6). It represents a change in the clasts source with the disappearance of the polymictic clasts and dark chlorite aggregates.

3.3. Sequence 3

Rocks from sequence 3 are bimodal in composition and clusters within the basalt/andesite and dacite/rhyolite fields of Pearce (1996) (Fig. 7a). Both group are macroscopically similar and can only be distinguished through geochemical analysis. Andesite (3_I) is dominant at the base of the sequence whereas dacite (3_F) is more common near the top of the sequence and are the primary host to the mineralisation (Figs. 5 and 6). Both andesite and dacite consists of poorly sorted monomictic breccias and flows, and are consistent with deposition in a vent proximal depositional setting (McPhie et al., 1993; Allen et al., 1996; Gibson et al., 1999).

The monomictic breccias contains >50% very fine-grained quartz and feldspar, a dark grey to dark blue matrix, disseminated pyrite (<3%), and large (>10 cm) intermediate to felsic clasts (Fig. 8fg). They consist of aggregates of monomictic, clast-supported, matrix-poor, poorly sorted volcanoclastic rocks that commonly grade into in situ jigsaw-fit breccia and massive flows. Individual breccia intervals correlate poorly between drill holes and appear to have irregular geometries and distributions. The

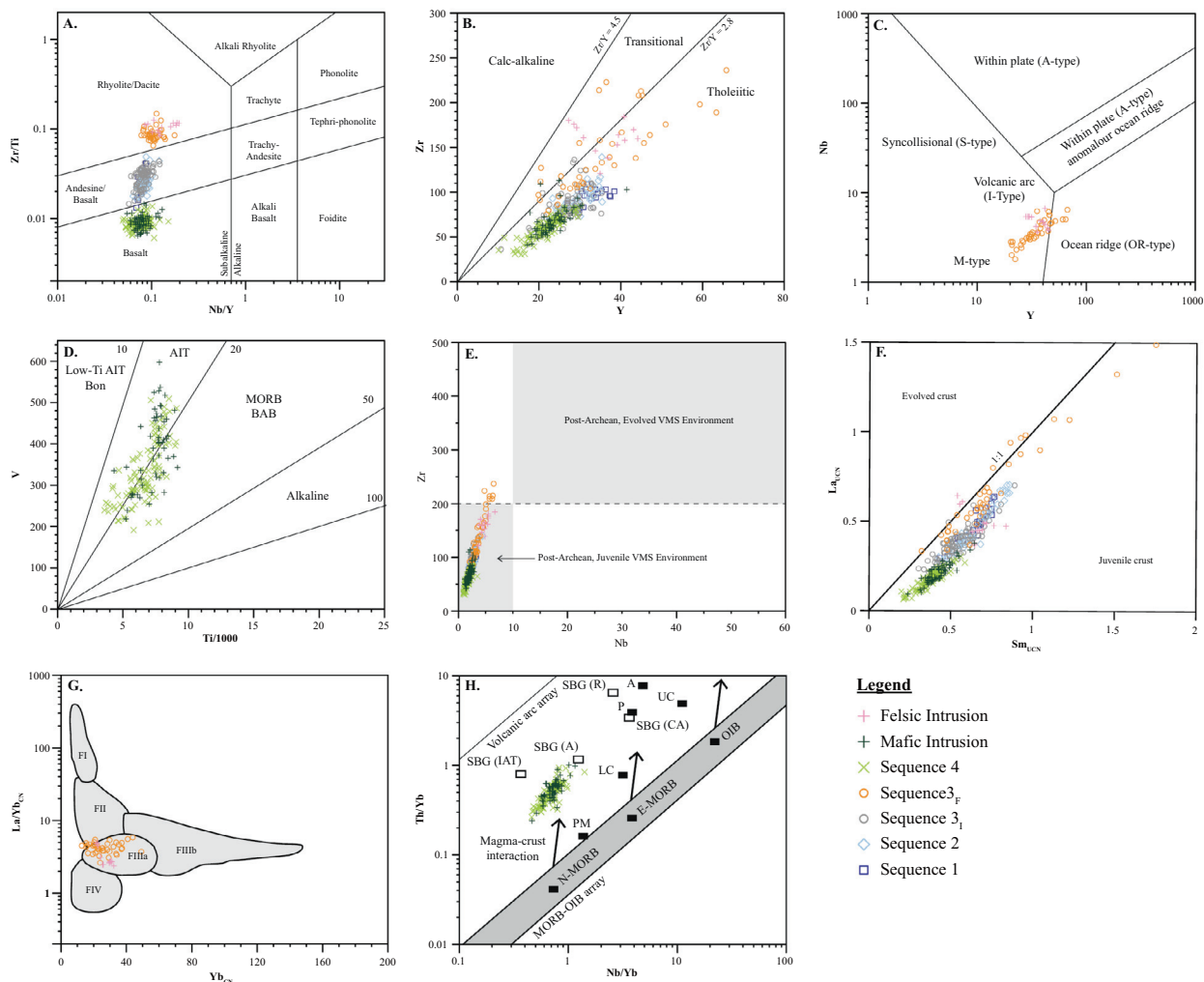


Fig. 7. Immobility element discrimination diagrams for the volcanic rocks from the Lemarchant area. (A) Zr/TiO₂-Nb/Y (Winchester and Floyd 1977) with modified field boundaries of Pearce (1996). (B) Zr-Y discriminating magma affinity with fields of Ross and Bedard (2009). (C) Nb-Y with field boundaries of Pearce et al. (1984) for felsic rocks. (D) V-Ti/1000 diagram with field boundaries of Shervais (1982) for mafic rocks. (E) Zr-Nb diagram of Piercey (2009) discriminating juvenile environments from evolved environments. (F) Upper-crust normalised (UCN) La-Sm diagram (normalisation values from McLennan, 2001). (G) La/Yb_{CN}-Yb_{CN} FI-FIV rhyolite discrimination diagram for chondrite normalised values (CN) from McDonough and Sun, 1995; diagrams from Lesher et al., 1986; and Hart et al., 2004). (H) Th/Yb-Nb/Yb diagram of Pearce (2008) for mafic volcanic rocks. Also shown in (H) are the average composition of the lower crust (LC), upper crust (UC), felsic Phanerozoic (P) and Archean (A) crust from Rudnick and Fountain (1995), and average composition of the Sandy Brook Group (SBG) island arc tholeiite (IAT), andesite (A), and rhyolite (R) from Rogers et al. (2006).

monomictic breccias are commonly overprinted by weak to strong sericite alteration. Veinlets of sphalerite, chalcopyrite, coarse quartz, chlorite and carbonate crosscut the monomictic breccias and early sericite alteration near mineralised intervals. However, late sericite veinlets also crosscut the sphalerite-chalcopyrite veinlets, suggesting at least two episodes of sericite alteration. It is unclear if the monomictic breccias are formed by synvolcanic autoclastic mechanisms or are the result of hydrothermal alteration of jigsaw-fit breccias on flow margins, transforming them into apparent pseudo matrix-supported breccia (Allen, 1988; McPhie et al., 1993).

The flows are flow-banded and jigsaw-fit flows that are white to creamy-yellow (Fig. 8hi). The groundmass consists of an intergrowth of quartz and feldspar with subordinate euhedral, <1 mm long, disseminated pyrite and anatase grains. Feldspar phenocrysts <2 mm long are also present in the groundmass and locally exhibit Carlsbad or albite twinning. Aphanitic dark grey to black chlorite with subordinate sphalerite, and chalcopyrite fills the interstices between the jigsaw pieces. Both flows commonly display varying degrees of late sericite and carbonate alteration.

Sequence 3 is commonly in structural contact with sequences 1 and 2 but is conformable with sequence 2 in section 106+00N (Fig. 5c). Sequence 3 rocks occur in every structural block at Lemarchant but are more predominant within the central and western portion of the Lemarchant property (Figs. 5 and 6).

3.4. Mineralisation and alteration

Lithofacies associated with the mineralised sequence include: exhalative mudstones, massive barite, massive to semi-massive sulphides, chaotic chlorite-carbonate alteration, chlorite alteration and sericite alteration. The mineralisation in both the Main and Northwest zones is hosted within the dacitic breccias and flows of sequence 3, with the exception of the exhalative mudstones, which overlay the rocks of sequence 3. Precise timing for the initiation of the Lemarchant VMS system is not known. However, cross-cutting relationships suggest that it was initiated after the emplacement of the dacitic flows of sequence 3_F and prior to the deposition of the basalts of sequence 4. Layers of exhalative mudstones are also present within the hanging wall basalts above the Main Zone attesting that the Lemarchant hydrothermal system



Fig. 8. Intermediate and felsic volcanic rocks the Lemarchant area. (A) Polymictic breccias with characteristic chlorite spots from sequence 1; sample LM11-51_393m. (B) Polymictic breccia with polymictic clasts from sequence 1; sample LM08-37_266m. (C) Felsic tuff from sequence 1; sample LM08-37_145.5m. (D) Polymictic breccias from sequence 2; sample LM13-82_041m. (E) Felsic tuff from sequence 2; sample LM14-98_175.0m. (F) Intermediate monomictic breccia from sequence 3_F; sample LM11-71_94m. (G) Felsic monomictic breccia from sequence 3_F; sample LM13-86_101m. (H) Intermediate jigsaw-fit flow from sequence 3; sample LM11-51_150.0m. (I) Felsic flow-banded flow from sequence 3_F; sample LM08-37_326.3m. All drill core samples are from NQ core (diameter = 47.6 mm).

was at least still partly active during the deposition of the lowermost basalts of sequence 4.

3.4.1. Mudstone

The mudstones commonly vary in thickness between 0.1 and 10 m but can be as thick as 23 m. They are brown to black in colour, finely laminated, graphitic, and contain various amounts of fine carbonaceous/organic-rich laminae intercalated with chert ± apatite and with sulphides layers and are commonly hydrothermal exhalites (Fig. 9ab; Lode et al., 2015, 2016). Sulphides are dominated by pyrite and pyrrhotite, with minor amounts of marcasite, chalcopyrite, sphalerite, arsenopyrite, and galena. There is an increase in the chalcopyrite, sphalerite and galena content with proximity to the massive sulphide (Lode et al., 2015). Pyrrhotite-rich mudstones are common near the contacts with mafic intrusions and may be related to desulphidation of pyrite during the emplacement of the mafic intrusions. In general, mudstones near the Main Zone are generally well preserved but locally display weak to moderate shearing (Fig. 9a). In contrast, mudstones at the Northwest Zone are commonly structurally complex and have been affected by tight to open folding and faulting (Fig. 9b).

3.4.2. Massive barite

Barite-rich intervals are found below the mudstones and vary in thickness between 2 and 25 m. Barite is white to dark blue-grey in

colour and occurs as granular massive barite and is locally bladed (Fig. 9c). Massive barite intervals replace the felsic and intermediate volcanic footwall rocks and is intergrown with, and replaced by sulphide mineralisation (Gill and Piercey, 2014; Gill et al., 2015, in press).

3.4.3. Massive to semi-massive sulphides

Massive to semi-massive sulphide lenses are up to 25 m thick and consist principally of white to yellow sphalerite with subordinate of pyrite, chalcopyrite and sulphosalts replacing the intermediate and felsic volcanic host rocks (Fig. 9de; Gill and Piercey, 2014; Gill et al. 2013, 2015, in press). Semi-massive sulphides occur as disseminated aggregates and veins localised on fragment margins of the jigsaw-fit fragments and along flow-banding in the more massive parts of flows (Fig. 9e). Semi-massive sulphides are associated with zones of moderate to strong chlorite, sericite and/or quartz alteration. Massive sulphides commonly occur above semi-massive sulphide zones but can locally occur below or within larger intervals of semi-massive sulphides.

In the Main Zone (along section 103+00N; Fig. 5a), a pipe-shaped mineralised zone is observed below the dacitic volcanic rocks of sequence 3_F and above the Lemarchant thrust in drill core LM11-61. In the Northwest Zone (along section 106+00N; Fig. 5c), the mineralisation occurs immediately below the LJ shear zone.

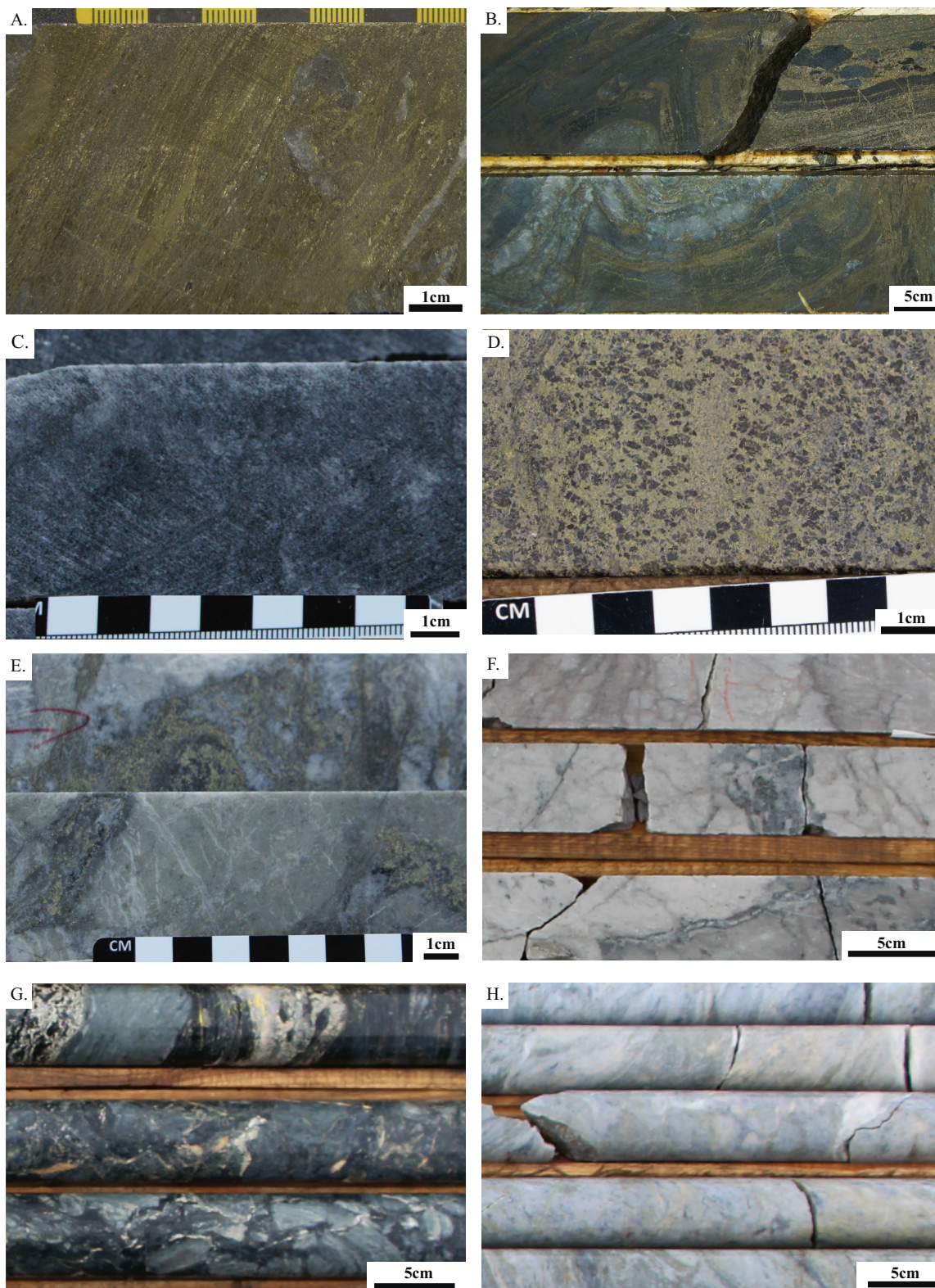


Fig. 9. Rocks associated with the Lemarchant VMS system (A) Weakly sheared exhalative mudstone sample from the Main Zone; sample LM11-68_196.95m. (B) Highly deformed and folded exhalative mudstone interlayered with tuff from the Northwest Zone; sample LM13-83_300.2m. (C) Unmineralised granular massive barite; sample LM13-73_336m. (D) Massive sulphides from the Northwest Zone consisting of chalcopyrite, sphalerite and pyrite; sample LM13-73_349.9m. (E) Semi-Massive sulphides from the Northwest Zone consisting of dissemination and veins of honey brown sphalerite and pyrite filling interstices among the jigsaw breccia fragments felsic flow. Weak chlorite, sericite and silica alteration occurs with the semi-massive sulphides; sample LM11-73_306m. (F) Silica alteration of an intermediate massive flow; sample LM13-82_336.3m. (G) Pervasive chlorite-carbonate alteration of a layered massive felsic flow; sample LM13-83_368.0m. (H) Sericite and silica altered felsic massive flow; sample LM13-87_356.3m. All drill core samples are from NQ core (diameter = 47.6 mm).

3.4.4. Alteration

Alteration in the Lemarchant deposit consists of chlorite-carbonate, chlorite, sericite, and silica alteration (Fig. 9fgh). Alteration varies from weak to strong and occur below the massive and semi-massive sulphide lenses. Chlorite ± carbonate alteration occurs within and below the semi-massive sulphide and generally overprints sericite alteration. Silica alteration occurs with both chlorite and sericite alteration or by itself. Carbonate alteration occurs within the massive sulphides and also extends several meters into the mafic volcanic rocks of the hanging wall.

3.5. Sequence 4

Sequence 4 consists of massive, pillowed, and amygdaloidal basalt and basalt breccias and falls within the basalt field of Pearce (1996) (Fig. 7a). The basalts lie conformably above the hydrothermal mudstones or the andesitic or dacitic volcanic rocks of sequence 3. They are restricted to the eastern portion of the Lemarchant property (Figs. 5 and 6).

3.5.1. Massive basalt

The massive basalts are aphanitic, dark grey to dark green with rare 0.5–2 mm feldspar and magnetite phenocrysts (Fig. 10a). They are crosscut by minor (up to 10%) 1–3 mm wide carbonate veinlets and 1–5 mm wide quartz-carbonate veinlets. Epidote alteration of the matrix is rare and restricted to within or immediately adjacent to fracture zones.

3.5.2. Amygdaloidal basalt

The amygdaloidal basalts are similar to the massive basalts but have 5–20%, 1–20 mm wide, rounded to sub-rounded carbonate filled amygdules (Fig. 10b). Chlorite replacement of carbonate in the amygdules occurs near fracture zones.

3.5.3. Pillow basalt

Intervals of pillow basalts consist predominantly of 5–50 cm wide pillows with rare pillows >50 cm in width. The pillows are aphanitic, dark grey to dark green, and contain 5–20% carbonate filled, 1–20 mm wide, rounded to sub-rounded amygdules (Fig. 10c). The amygdules are generally smaller and more elongated towards the edge of the pillow where they are 1–2 mm wide. Inter-pillow volcano-sedimentary rocks consist of a mixture of very fine-grained basalt, epidote, white mica, carbonate, and pyrite. The pillow basalts are crosscut by moderate amounts (up to 10%) of 1–3 mm wide carbonate veinlets and 1–5 mm wide quartz-carbonate veinlets. Both the pillows and interflow sedimentary rocks commonly have weakly to moderately developed epidote and carbonate alteration.

3.5.4. Basalt breccia

The basalt breccias are highly variable in texture and vary between jigsaw-fit, fragment- to matrix-supported-breccia. Fragments consist of aphanitic, dark green to dark grey basalt that vary in size between 0.5 and 10 cm (Fig. 10d). The matrix varies between carbonate dominated to epidote ± carbonate dominated.

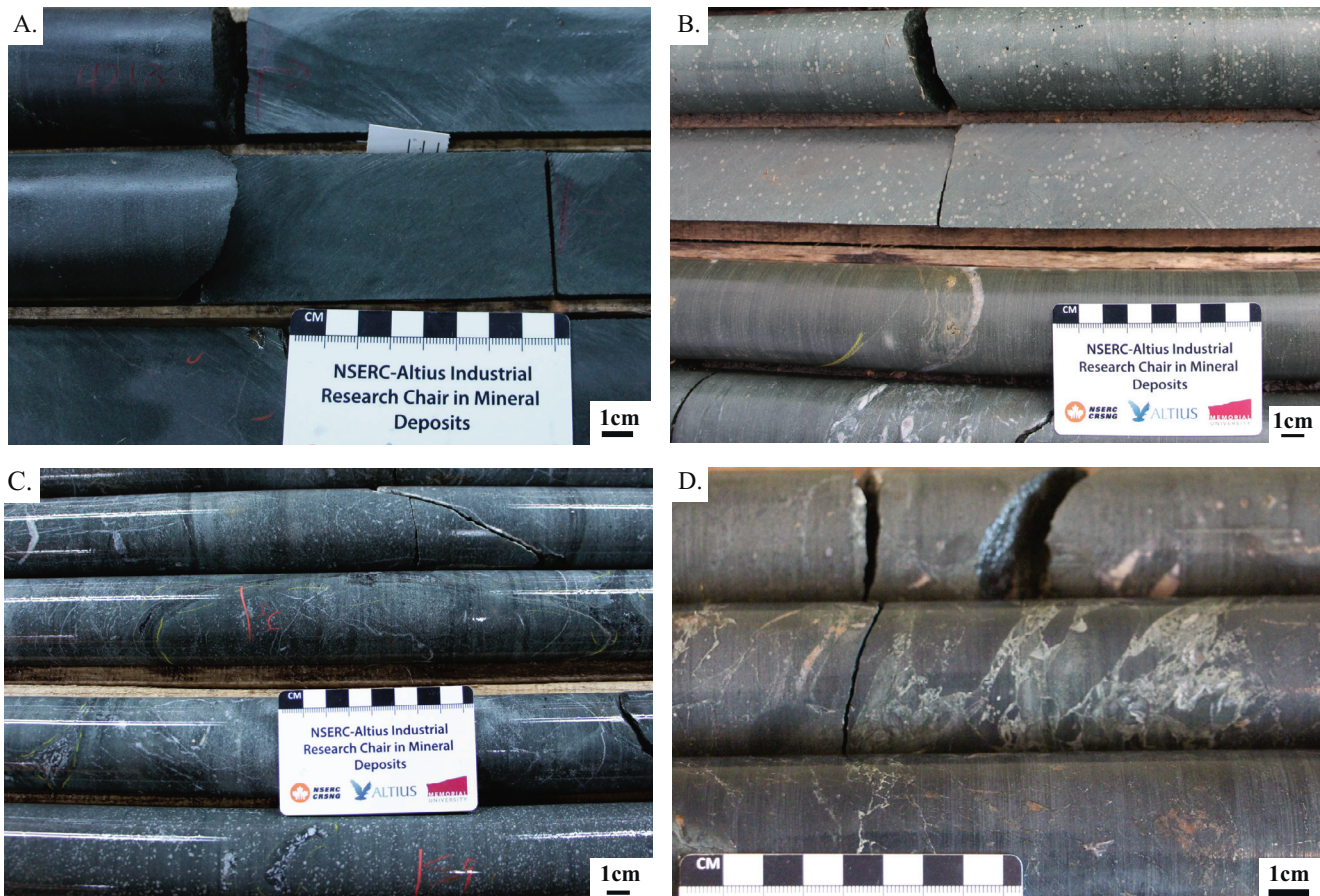


Fig. 10. Mafic rocks from sequence 4. (A) Massive basalt; sample LM11-49_421.3m. (B) Amygdaloidal basalt; sample LM07-16_106m. (C) Pillow basalt; sample LM11-49_056m. (D) Basalt breccia; sample LM07-16_046.2m. All drill core samples are from NQ core (diameter = 47.6 mm).

3.6. Intrusions

Three types of intrusions have been identified in the Lemarchant area, including: mafic, intermediate and felsic intrusions.

3.6.1. Mafic intrusions

Mafic intrusions are macroscopically similar to the amygdaloidal basalts of sequence 4 and fall within the basalt field of Pearce (1996) (Fig. 7a). They are aphanitic, dark grey to dark green to grey-beige in colour, contain 10–25% of 1–20 mm carbonate-filled amygdules (Fig. 11a). The mafic intrusions locally exhibit sharp chilled contact margins, which make them difficult to identify when intruding mafic extrusive rocks of sequence 4. However, the intrusions can be recognised by their significantly lower amounts (<1%) of carbonate or quartz veinlets. Likewise, the mafic intrusions and locally contain 20–40 mm long euhedral pyrite

cubes which are absent in the mafic extrusive rocks. The mafic intrusions cross-cut rocks from all sequences and rare <10 m sills occur within the mafic rocks of sequence 4. Trace element composition of the mafic intrusions is indistinguishable from the mafic extrusive rocks of sequence 4 (Fig. 7), and suggests that the emplacement of the mafic intrusions might have been in part synchronous or genetically related with the deposition of the mafic volcanic rocks of sequence 4.

3.6.2. Felsic intrusions

Two types of felsic intrusions with chemistries clustering within the dacite/rhyolite fields of Pearce (1996) are present at Lemarchant (Fig. 7a). The first type is cream coloured and contains <20%, 2–5 mm wide, feldspar phenocrysts hosted in quartz-rich groundmass that locally exhibit chilled contact margins (Fig. 11c). The second type is volumetrically subordinate (<0.5% of total rock volume) and consists of 20–50%, 1–3 mm long, white feldspar phenocrysts hosted in a creamy-white to pink groundmass. These intrusions are commonly <5 m wide, exhibit sharp chilled margins with surrounding rocks and occur within or proximal to shear zones. The felsic intrusions crosscut every sequences present in the Lemarchant area, including the mineralisation and alteration sequence. However, they are commonly spatially associated with the felsic rocks of sequences 1–3 and are not volumetrically abundant in the mafic volcanic rocks of sequence 4.

3.6.3. Intermediate intrusions

The intermediate intrusions contain <15%, 1–4 mm wide, white feldspars phenocrysts hosted in a pale grey groundmass (Fig. 11b). Intermediate intrusions are volumetrically minor, accounting for <1% of the rocks present at Lemarchant. These intrusions are not spatially associated with the mineralisation and are only recognised as cross-cutting bodies in sequence 4 in drill cores LM11-49 and LM11-50 on section 108+00N.

4. Lithochemistry

A total of 794 samples of all rock, alteration and mineralisation types from the Lemarchant area were collected from 46 diamond drill cores. Major oxides (SiO_2 , Al_2O_3 , Fe_2O_3 , MnO , MgO , CaO , Na_2O , K_2O , TiO_2 , P_2O_5) were analysed at ALS Global following the ME-XRF06 method in which 0.9 g of sample was added to 9.0 g of lithium borate Flux (50–50% $\text{Li}_2\text{B}_4\text{O}_7$ – LiBO_2), mixed well and fused into a glass disc with an auto fluxer between 1050 and 1100 °C, and analysed by X-ray fluorescence spectroscopy (XRF). Lower detection limits are 0.01% for all of the major oxides. Trace elements were analysed on 371 samples at ALS Global following the ME-MS81 method in which 0.2 g of crushed sample is added to 0.9 g of lithium metaborate ($\text{Li}_2\text{B}_4\text{O}_7$), mixed well and fused in a furnace at 1000 °C. The resulting melt was cooled and dissolved in 100 mL of 4% HNO_3 and 2% HCl solution, and was analysed by inductively coupled plasma mass spectrometry (ICP-MS). Lower detection limits varied between 0.01 and 10 ppm, with most elements having detection limits below 1 ppm.

Most host rocks in VMS systems are altered to some extent (e.g., Large, 1977; Franklin et al., 1981, 2005; Lydon, 1984, 1988; Hannington, 2014), restricting the elements that can be used for understanding the primary lithochemical signatures of host rocks. Immobile elements such as Al, Ti, the high field strength elements (HFSE) and the REE (except Eu) are ideal to provide information on the primary petrochemical attributes of the rocks in VMS systems. However, caution must be used as some of these element may become mobile (especially the LREE) during intense hydrothermal alteration (MacLean, 1988).

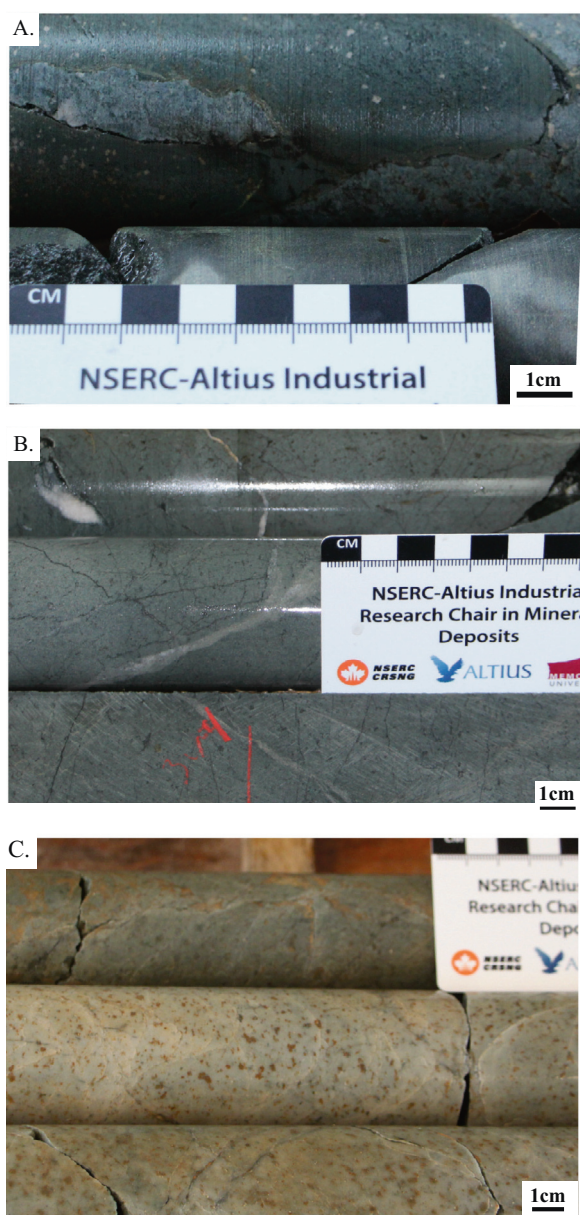


Fig. 11. Intrusions from the Lemarchant area. (A) Mafic intrusion; sample LM08-37_108.4m. (B) Intermediate intrusion; sample LM11-49_343m. (C) Felsic intrusion; sample LM08-34_318m. All drill core samples are from NQ core (diameter = 47.6 mm).

4.1. Mobile element systematics

Rocks from the Lemarchant area display weak to strong alteration. Overall, $\text{Al}_2\text{O}_3/\text{Na}_2\text{O}$ ratios (Fig. 12a; Spitz-Darling index, Spitz and Darling, 1978) are generally lower than 20, indicating low levels of alteration. However, samples with $\text{Al}_2\text{O}_3/\text{Na}_2\text{O}$ ratios as high as ~50 occur in sequences 3₁, and 4 and in the mafic intrusion. Samples with $\text{Al}_2\text{O}_3/\text{Na}_2\text{O}$ ratios as high as 235 occur in sequence 3_F, indicative of strong alteration. Plot of AI index ($\text{AI} = 100 * (\text{MgO} + \text{K}_2\text{O}) / (\text{MgO} + \text{K}_2\text{O} + \text{CaO} + \text{Na}_2\text{O})$; Ishikawa et al., 1976) versus chlorite-carbonate-pyrite index ($\text{CCPI} = 100 * (\text{MgO} + \text{Fe}_2\text{O}_3) / (\text{MgO} + \text{Fe}_2\text{O}_3 + \text{CaO} + \text{Na}_2\text{O})$; Large et al., 2001), rocks from sequences 1, 2 and 3, and the felsic intrusions plot in both the least altered and the altered fields, whereas rocks from sequence 4 and the mafic intrusions plot only in the least altered field (Fig. 12b). Felsic and intermediate samples that plot in the altered field display moderate to high AI and CCPI indexes, and vary between the least altered, the sericite and the chlorite fields. In addition, some felsic volcanic rocks from sequence 3 and felsic intrusion have high Na_2O values (Fig. 12a) and plot near the albite field in the AI versus CCPI diagram (Fig. 12b).

4.2. Immobile element systematics

Most rocks fall within the tholeiitic field of Ross and Bedard (2009) (Fig. 7b) with rocks from sequences 1, 2, 3₁, 4, and the mafic intrusions defining a cluster with Zr/Y ratios ranging from 1.9 to 5.3, and dacitic rocks from sequence 3_F defining another cluster with higher Zr/Y ratios ranging from 3.2 to 5.5. Felsic intrusions have even higher Zr/Y ratios ranging from 3.5 to 6.6, indicating a tholeiitic to transitional affinity (Fig. 7b). The dacites of sequence 3 and the felsic intrusions plot in the volcanic arc field on the Nb-Y discrimination diagram of Pearce et al. (1984) (Fig. 7c), whereas the mafic rocks of sequence 4 and the mafic intrusions plot on the boundary between the island arc tholeiite and the mid-ocean ridge basalt (MORB)/back-arc basalt (BAB) fields on the Ti-V discrimination diagram of Shervais (1982) (Fig. 7d).

All the samples have low Zr (<200 ppm) and Nb (<10 ppm) contents (Fig. 7e), upper crust-normalised La/Sm ratios <1 (McLennan, 2001; Fig. 7f), and are consistent with input from juvenile crust/mantle (Piercey, 2010, 2011). In addition, most samples fall within the FIIa field (Fig. 7g) of Lesher et al. (1986) and Hart et al. (2004),

indicating that partial melting likely took place at relatively shallow levels (<10 km) in the crust. However, the basalts from sequence 4 and the mafic intrusions suggest crustal contamination and/or slab fluid influence based on the Th/Yb-Nb/Yb discrimination diagram of Pearce (2008) (Fig. 7h).

4.3. Primitive mantle normalised plots systematics

The extended trace element profiles for each sequence has been normalised to relative to the primitive mantle values of Sun and McDonough (1989). Overall, every sequence has negative Nb, Ti, and Zr anomalies (Fig. 13). Intermediate volcanic rocks of sequences 1, 2 and 3₁ have similar extended trace element profiles and are enriched in light REE compare to heavy REE, with negative Nb and Ti, moderate negative Zr anomalies (Fig. 13a-c). The dacite of sequence 3_F is enriched in light REE, has strong negative Nb and Ti anomalies and moderately negative Zr anomalies (Fig. 13d). The profiles are similar to the profiles of intermediate volcanic rocks from sequences 1, 2 and 3₁ but the dacite exhibits more pronounced negative Ti anomalies. Felsic intrusions have similar profiles to the dacite of sequence 3_F but generally contain higher absolute values of trace elements (Fig. 13e). Basalts from sequence 4 and the mafic intrusions have similar flat extended trace element profiles, characterised by strong negative Nb anomalies, and moderately negative Zr and Ti anomalies (Fig. 13fg).

5. Structural elements

Structural elements in the Lemarchant area consist of fractures, gouge, shear zones, and faults. Fracture zones range from 10s of centimetres to 10s of meters and consist of sharp sets of dense to widely spaced parallel fractures. The fractures are generally open with no visible alteration on their surfaces, except in rare cases where the fracture surfaces and the adjacent bedrock is bleached up to 1 cm into the wallrock. The majority of fractures have smooth surfaces indicating minimal displacement along them; however, fracture surfaces locally show slickenlines, indicating some displacement. Within the fault zones, areas with the maximum intensity of deformation manifest themselves as 5–25 cm wide zones of bleached fault gouge. Fracture zones are present in every rock unit at Lemarchant.

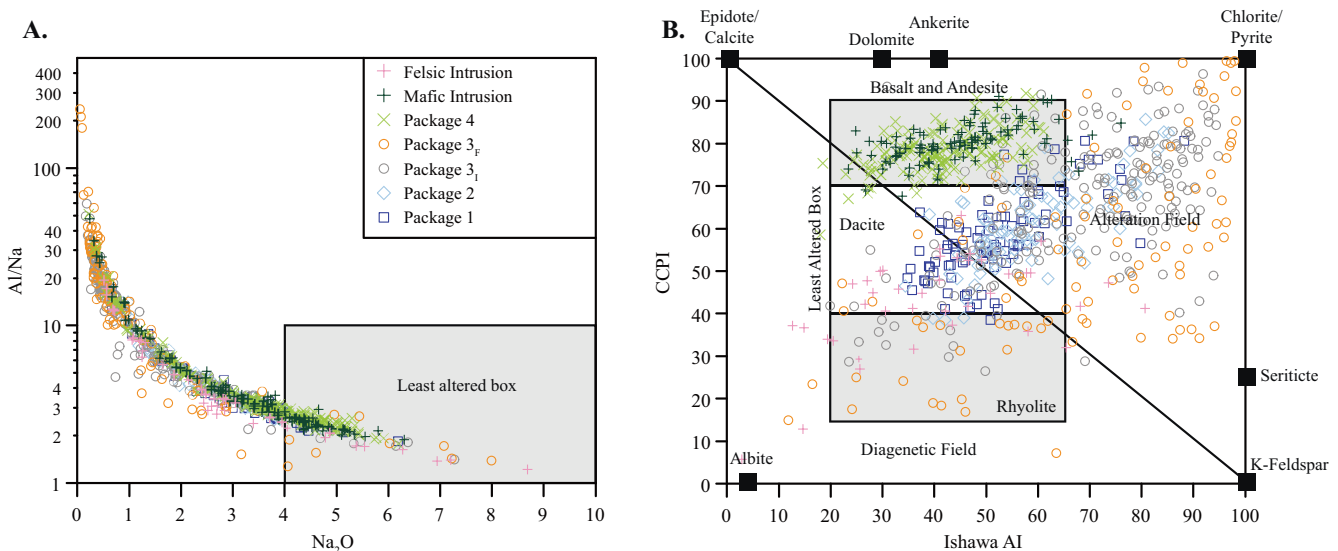


Fig. 12. Mobile element plots for the rocks from the Lemarchant VMS deposit. (A) Spitz-Darling (Spitz and Darling 1978) index versus Na_2O (diagram after Ruks et al. 2006). (B) Alteration box plot with the AI index (AI; Ishikawa et al. 1976) plotted against the chlorite-carbonate-pyrite index (CCPI; Large et al. 2001).

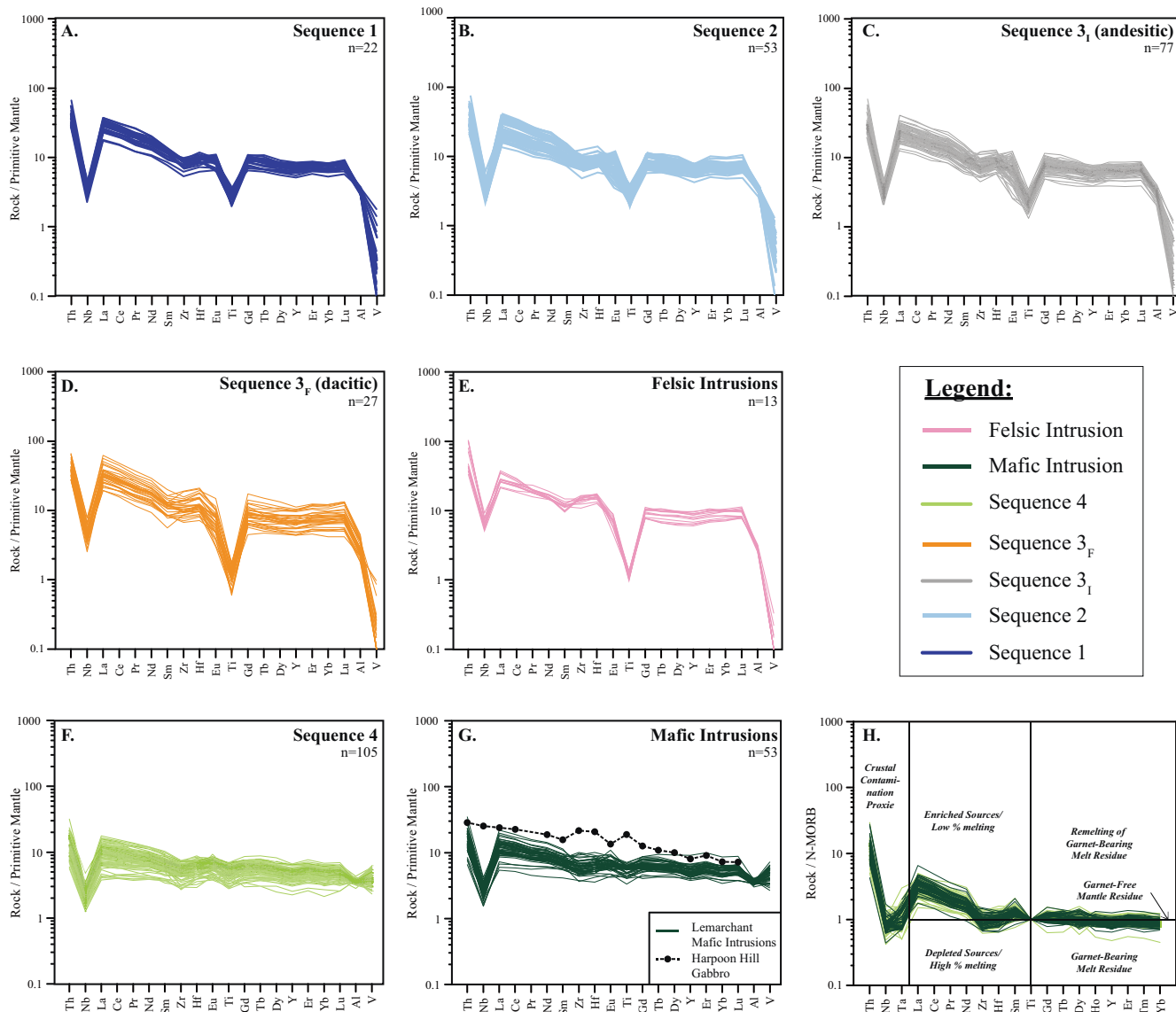


Fig. 13. Primitive mantle normalised extended REE element profiles for the rocks from the Lemarchant area. (A) sequence 1, (B) sequence 2, (C) sequence 3₁ (andesitic), (D) sequence 3_F (dacitic), (E) felsic intrusions, (F) sequence 4, (G) mafic intrusions, and (H) mafic volcanic rocks normalised to N-MORB, and subsequently renormalised to Ti (Ti = 1) with the tectonic fields of Pearce (2008). In all, normalisation factors are from Sun and McDonough (1989).

Shear zones consist of moderately to highly foliated ductile to brittle shears. They vary in thickness from 10 cm to 10s of meters, depending on the competence of the rocks and the deformation intensity. The main shear zones recognised during this study are termed the LJ, KJ and Lemarchant shear zones, whereas the Bam fault is the only extensional fault recognised in the study area (Fig. 6).

5.1. LJ shear zone

The LJ shear zone is a southeast striking shear zone dipping at ~60° towards the southwest (Fig. 6). It typically ranges in thickness from 0.5 to 7 m, but can locally be up to 25 m in thickness. It occurs exclusively within rocks of sequence 3 and thrusts the non- to weakly-mineralised rocks of the hanging wall over the non- to highly-mineralised rocks of the footwall. The LJ shear zone has been folded into open folds during post-VMS deformation (Fig. 6). A late mafic intrusion, herein referred to as the Pacman intrusion, was emplaced in the axis of the LJ shear zone in between section 104+50N and 106+50N, healing and masking portions the

LJ shear zone in these areas. The LJ shear zone and the Pacman intrusion are cross-cut by the Lemarchant shear zone (Fig. 6).

5.2. KJ shear zone

The KJ shear zone is parallel to and located ~10 to 35 m above the LJ shear zone (Fig. 6). The KJ shear zone varies in thickness between 0.4 and 8 m and thrusts rocks from sequences 1 and 2 over non- to weakly-mineralised rocks of sequence 3. As it is the case for the LJ shear zone, the KJ shear zone has been affected by open folding during post-VMS event deformation, and was intruded by the Pacman intrusion between sections 104+50N and 106+50N is crosscut by the Lemarchant shear zone (Fig. 6).

5.3. Lemarchant shear zone

The Lemarchant shear zone is an extensive, relatively flat, horizontal shear zone that occurs throughout the Lemarchant property (Fig. 6). On average, it ranges between 1 and 10 m in thickness but is locally up to 30 m thick. The Lemarchant shear zone is offset by

the Bam fault in the central portion of the property between section 104+00N and 105+00N. The observed depth of the Lemarchant shear zone is approximately 200 m above the mean sea level north of the Bam fault and 100 m above the mean sea level south of the Bam fault. The Lemarchant shear zone is not significantly affected by folding and crosscuts both the LJ and KJ shear zones.

5.4. Bam fault

The Bam fault is an east striking fault dipping at $\sim 60^\circ$ towards the south and ranges in thickness between 1 and 10 m (Fig. 6). It crosscuts the LJ, KJ and Lemarchant shear zones. The Bam fault records a normal-sense of displacement wherein the rocks south side of the fault was down-faulted relative to the north side. Relative movement is estimated to be around 100 to 150 m based on the offset of the Lemarchant shear zone (Fig. 6).

6. Discussion

6.1. Tectonic evolution of the Lemarchant host rocks

All sequences and intrusions examined in this study exhibit similar primitive mantle normalised extended REE profiles with negative Nb, Zr, and Ti anomalies (Fig. 13), suggesting a similar tectonic environment of formation. In general, negative Nb, Zr, and Ti anomalies are characteristic of “arc” environments, where slab metasomatism has influenced the overlying mantle wedge resulting in an enrichment of large ion lithophile elements relative to high field strength elements (e.g. Hawkesworth et al., 1993; Pearce and Peate, 1995; Piercey, 2010). This “arc” signature is also supported in the Ti-V systematic of the basalts and mafic intrusions (Fig. 7d), where they cluster near the boundary between the island arc and back-arc/MORB fields. Additional support for the “arc” signature can be seen in Th/Yb and Nb/Yb discrimination diagram where basalt and mafic intrusions plots above the MORB-OIB array with elevated Th/Yb at a given Nb/Yb (Fig. 7h), indicating either the influence from slab metasomatism or crustal contamination during ascent. In addition, the dacite and felsic intrusions plot in the volcanic arc field on the Y versus Nb discrimination diagram of Pearce et al. (1984) (Fig. 7c), further supporting the arc environment interpretation.

Despite the evidence for an arc environment, the majority of the Lemarchant samples have a tholeiitic affinity (Fig. 7b), exhibit juvenile signatures compare to typical upper continental crust ($La/Sm_{UCN} < 1$; Fig. 7f) and plots in the post-Archean juvenile VMS environment field on the Nb versus Zr discrimination diagram of Piercey (2011) (Fig. 7e). Furthermore, the rocks at the Lemarchant area do not exhibit a continuous spectrum of magmatic products, features common in most “arc” environments (e.g., Tatsumi and Eggins, 1995), but rather are bimodal to trimodal in nature, features commonly observed in rifted arc environments (e.g., Vivallo and Claesson, 1987; Wright et al., 1996), and consistent with regional tectonics models (e.g., Rogers et al., 2006; Zagorevski et al., 2010; Piercey et al., 2014). However, it should be noted that some areas of the Tally Pond group (e.i., West and South Tally Pond zones) exhibit a continuous spectrum of magmatic products fractionation (Pollock, 2004). The FIIIa signature of the dacite and felsic intrusions at the Lemarchant area (Fig. 7g) supports a shallow melting environment (< 10 km), with melting taking place under low pressure (< 0.5 Gpa) and high temperature (900–1000 °C) (Fig. 7e; Lesher et al., 1986; Hart et al., 2004; Piercey, 2011). Similarly, the extended REE profiles normalised to N-MORB and Ti suggest shallow melting from a garnet free and spinel stable residue for the basaltic melts of sequence 4 (Fig. 13h; e.g., McKenzie and Bickle, 1988; McKenzie and

O’Nions, 1991; Pearce, 2008). Therefore, the arc signatures present at Lemarchant area are interpreted to be the direct result of slab metasomatism (e.g., Hawkesworth et al., 1993; Pearce and Peate, 1995), and/or inherited from contamination via arc crust (e.g., Morris et al., 2000) or continental crust assimilation (e.g., Piercey et al., 2004). The interpreted volcano-sedimentary environment at the Lemarchant area and the regional tectonic models and are consistent with continental crust assimilation during magma ascent.

The Tally Pond group is underlain by the 563 Ma Sandy Brook group, which consists of rhyolite, andesite and basalt (tholeiitic and calc-alkaline), and minor siliciclastic rocks, including black shale and chert horizons (Rogers et al., 2006). These rocks have evolved Nd isotopic signatures (ϵNd_{563Ma} from -5.18 to -0.67) and are interpreted to have formed within a continental arc environment (Rogers et al., 2006; Zagorevski et al., 2010). Evidence of relatively young, but evolved crust beneath the Tally Pond group at the Lemarchant deposit is also found in the Pb isotopic signatures of galena from the mineralised zones (Gill et al., 2015; Gill, 2015). Therefore, it is plausible that the “arc” signatures present in some of the rocks were at least in part inherited from interaction with the underlying arc basement (i.e., the Sandy Brook group). Despite being underlain by young arc crust, the presence of arc tholeiitic rocks with “juvenile” like signatures is indicative of the magmas erupting rapidly with limited interaction with crust during its ascent and is consistent with rifted arc and VMS formation environments (e.g., Piercey, 2011).

Several models have been proposed for the tectonic setting for the Tally Pond group. Dunning et al. (1991) argued that the Tally Pond group was the product of arc volcanism created by subduction zone magmatism in an oceanic setting. Rogers et al. (2006) claimed that the Tally Pond belt formed from subduction along the peri-Gondwanan side of Iapetus. However, they argue that the Tally Pond volcanic arc was built on the Ganderian microcontinent (Sandy Brook group – Crippleback Intrusive Suite crust) and not in an oceanic setting as proposed by Dunning et al. (1991). Based on Nd isotopes, Rogers et al. (2006) proposed that the Tally Pond belt formed from 60% juvenile depleted mantle and 40% recycling of older crust. In contrast, Zagorevski et al. (2010) hypothesised that the arc signature of the Tally Pond belt was the result of eastward subduction creating local arc volcanism within a greater extensional back-arc complex in which the magmatic front migrated westward with time due to slab rollback. In this model, these extensional eruptive complexes are associated with longitudinal rifts crosscut by cross-arc seamount chains. Similarly, Piercey et al. (2014) argues that the Duck Pond and Boundary deposits formed within a rifted arc environment along the edge of the Ganderian margin of the Iapetus ocean. More recently, Lode et al. (2016) suggested a two-phase rifting model for the Tally Pond group wherein the Lemarchant deposit formed at shallow depth during phase one of rifting.

Our model for the Lemarchant area agrees with the young rifted arc environment of Zagorevski et al. (2010), Piercey et al. (2014) and Lode et al. (2016) and explain the abundance of rocks with a juvenile geochemical signatures, the distinctly trimodal signature of the belt comparatively to dominantly andesitic with continuous fractionation trends (basalt to rhyolite) for continental arcs (e.g., Arculus, 1994; Lentz, 1998; Swinden, 1996), and is consistent with the extensional environment of formation of VMS deposits comparatively to compressive environments for arcs (Fig. 14) (e.g. Franklin et al., 2005; Galley et al., 2007; Piercey, 2010, 2011; Hannington, 2014). However, since continuous magmatic products are observed within the Tally Pond group (Pollock, 2004), compressive arc environments were also locally present.

Due to the high abundance of andesite compared to the bimodal (basalt and rhyolite) sequence at Duck Pond and elsewhere in the

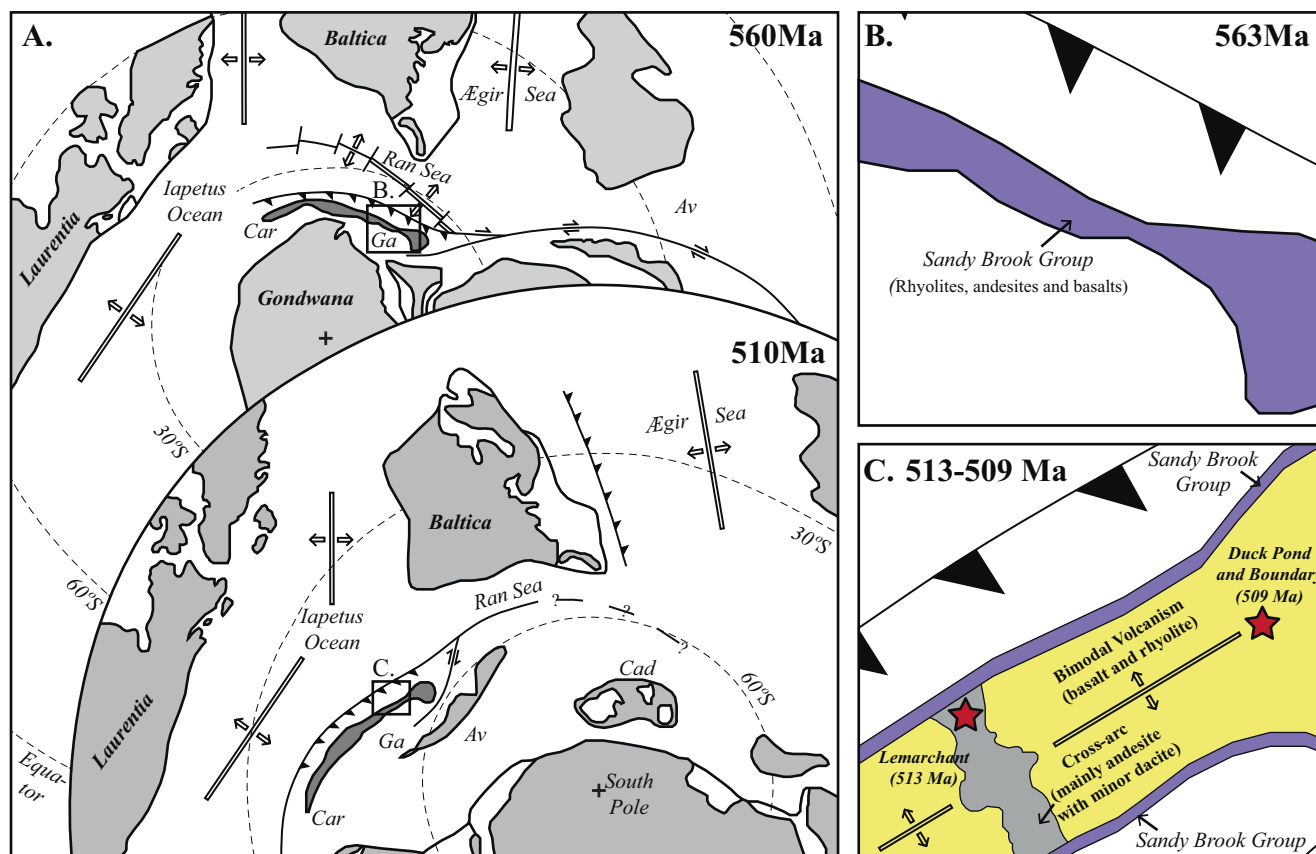


Fig. 14. Neoproterozoic to middle Cambrian paleogeographic reconstructions of the distribution of the continental landmasses within the southern hemisphere (modified from Rogers et al., 2006). (A) The Lemarchant deposit likely formed in southern latitudes in a peri-Gondwanan setting along the edge of Ganderia. The location of the potential environment of the Lemarchant deposit is outlined in the black box. (B) Early stage (563 Ma). Formation of the Sandy Brook Group within a magmatic arc. (C) syn-mineralisation stage (513–509 Ma). Rifting of the 563 Ma Sandy Brook Group magmatic arc and emplacement of the Tally Pond Group within the rifted zone. The Lemarchant deposit likely formed within a migrating cross-arc at shallow water depth (<1500 m below sea level), which permitted the hydrothermal fluid boiling and deposition of precious metals. Abbreviations are as follow: Av: Avalonia; Cad: Cadomia; Car: Carolina Terrane; and Ga: Ganderia (darker grey shading).

Tally Pond belt (Fig. 14c), we propose that the Lemarchant deposit formed either at an arc front or within a migrating cross-arc. A similar tectonic environment has been observed by Wright et al. (1996) within the modern Havre Through, north of the Taupo Volcanic Zone, wherein east-west andesitic arcs and associated cross-arcs occur perpendicular to the main north-south arc axis. Wright et al. (1996) suggested that the cross-arcs formed during the eastward migration of the subduction and associated arc magmatic fronts, and highlight areas where andesitic arc magma supply is greater than the rifting rate. Following this model, we hypothesise that the Lemarchant deposit formed following the attenuation of the andesitic arc magma supplies, likely when the rift-related magma supply became dominant. This transition was accompanied by a change from andesitic to dacitic magmatic composition during deposition of sequence 3 due to either mixing of the andesitic arc magma with rhyolitic magmas derived from the rift component or by crustal assimilation within the andesitic arc or cross-arc, creating the sparse dacite that host the VMS mineralisation. Subsequent to the transition to a rift dominated environment, the basalts of sequence 4 erupted over the andesitic and dacitic rocks of sequence 3. Hydrothermal activity related to the Lemarchant deposit continued during that time (i.e., post-VMS formation) as attested by the presence of interlayered exhalative mudstones within the basalts (Lode et al., 2015, 2016).

The relatively shallower position of VMS systems formed at the front of or within the magmatic cross-arcs compared to those formed at greater depths (i.e., in rift basins) may have enhanced boiling and allow enrichment in precious metals. At Lemarchant,

potential boiling is evidenced by abundant sulphosalts (i.e., tetrahedrite-tennantite), electrum, bladed barite, Ca-Fe-Mg-Mn-carbonate, and enrichments in epithermal suite elements (i.e., Au, As, Bi, Co, Cr, In, Mo, Ni, Sb, Se, Te; Gill et al., 2013, 2015; Gill and Piercey, 2014; Lode et al., 2015). Based on the ore mineralogy of the Main Zone at Lemarchant, Gill et al. (2015, in press) suggested that the deposit formed from intermittent boiling of hydrothermal-magmatic fluids at relatively shallow (<1500 m) water depth, and is consistent with the model propose therein. Boiling of Au-bearing magmatic fluids may have aided or may have been critical to the precious metal enrichment at the Lemarchant VMS system. Boiling resulted in a fluid phase with decreased HS⁻ activity due to strong fractionating of H₂S into the vapour phase, increased pH as a result of acidic components fractionating into the vapour phase, and decreased temperature (William-Jones et al., 2009). These promotes the destabilisation of the precious and base metal complexes in solution and result in their precipitation at the site of boiling.

6.2. Structural evolution of the Lemarchant area

The Lemarchant area was affected by several episodes of deformation following the deposition of sequences 1–4 and the VMS mineralisation hosted therein. Recorded deformation is more intense within the mudstone near the shear zones and within sheared massive sulphides of the Northwest Zone. It is proposed that the LJ and KJ shear zones originated as are syn-volcanic structures as both shear zones are found at ~45° to the stratigraphy

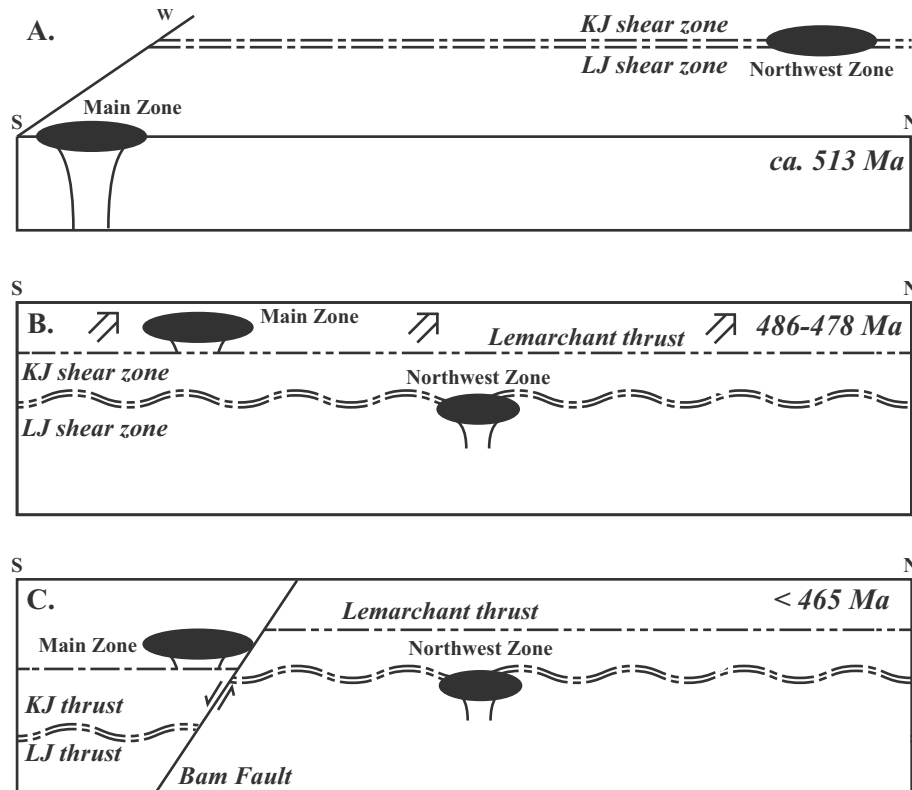


Fig. 15. Geotectonic evolution of the Lemarchant area. (A) Formation stage (513–509 Ma). The Main Zone and the Northwest Zone forms on or near the seafloor. (B) Main deformation stage (485–478 Ma). The LJ and KJ syn-volcanic shear zones are deformed and the Lemarchant thrust is emplaced thrusting the Main zone on the south of the current location of the Northwest Zone. (C) Late deformation stage (<465 Ma). Normal extension episode marked by the creation of the west striking Bam normal fault.

(Fig. 5c), and have different geometry (affected by early folding) compared to regional thrust faults in the area (Figs. 5c, 6, 15; e.g., McNicoll et al., 2010; Zagorevski et al., 2010). The kinematic indicators of the LJ and KJ shear zones suggest that older rocks of sequences 1 and 2 are thrust over younger rocks of sequence 3 and records an overall net reverse motion, indicating late reactivation of the syn-volcanic faults (Figs. 5c, 6, 13). Within the LJ shear zone, red sphalerite crosscut intervals of massive fine-grained, honey brown sphalerite and chalcopyrite, and is spatially associated with small aggregates of rounded to subrounded chalcopyrite. These textural relationships indicate that sphalerite deformed ductility and was remobilised parallel to LJ and KJ shear zones, whereas chalcopyrite was mechanically transported and concentrated into aggregates, as sphalerite does not require as high a pressure/temperature, relative to chalcopyrite, to reach the brittle-ductile transition and be ductility remobilised (Marshall and Gilligan, 1987). Consequently, from the sulphide relationship observed, it can be estimated that the pressures and temperatures reached during the deformation of the Lemarchant area did not exceed 175 MPa and 200 °C, respectively (Marshall and Gilligan, 1987). The high angle LJ and KJ syn-volcanic shear zones are crosscut by the relatively flat-laying Lemarchant shear zone (Figs. 5, 6, 13b) and suggests that the two mineralised zones did not originate from the same lens prior to deformation (Figs. 5 and 6). These observations are in agreement with those compiled by Squires and Hinchey (2006), suggesting that the Lemarchant shear zone is a thrust fault. On a regional scale, the Lemarchant thrust zone terminates against felsic rocks of the Bindons Pond formation which are crosscut by the nearby 465 ± 1 Ma (U–Pb zircon; Pollock 2004) Harpoon Hill gabbro (Squires and Hinchey, 2006) and possibly constrains the timing of the main deformation phases to the Penobscot orogeny (486–478 Ma; Colman-Sadd et al., 1992;

van Staal, 1994; Johnson et al., 2009; Zagorevski et al., 2010). In the eastern portion of the Exploits Subzone, east of the Tally Pond group, the Penobscot orogeny was accompanied by thrusting of locally derived Penobscot back-arc basin ophiolites onto the passive margin of Ganderia (Colman-Sadd, 1985; Colman-Sadd et al., 1992; Jenner and Swinden, 1993; Zagorevski et al., 2010). It is suggested that the Penobscot orogeny coincided with a NW-SE compression event in the Lemarchant area, that resulted in thrusting rocks over a few kilometres, as is the case for the obducted ophiolites in the east of the Exploits Subzone, and was accompanied by folding of the LJ and KJ syn-volcanic shear zones (Fig 15b; Colman-Sadd, 1985; Jenner and Swinden, 1993; Zagorevski et al., 2010).

The last deformation event recorded in the Lemarchant area corresponds to an episode of extension marked by the creation of the west striking Bam normal fault (Figs. 4, 15c). Regional mapping compilation conducted by Squires and Hinchey (2006) and logging of drill core south of the Main Zone suggests that the Bam normal fault is part of a series of NW-SE striking late normal faults that affected the southwest and northeast parts of the Tally Pond group. The timing of the late normal faults is unclear; however McNicoll et al. (2010) argues that late normal faults at Duck Pond displace a gabbro intrusion with a chemical signature similar to the Harpoon Hill Gabbro from which an age younger than 465 Ma can be inferred for the late normal faults. By analogy, the late relative timing for the normal faults at Lemarchant may suggest a maximum age of 465 Ma for normal faults, potentially related to an episode of tectonic relaxation post-Penobscot orogeny.

6.3. Implications for VMS exploration

Exploration for VMS deposits in accretionary orogenic belts is challenging due to post-VMS tectonic imbrication of original basin

sequences (e.g., Calon and Green, 1987; McClay, 1995; Thurlow, 1996; Nelson, 1997; Castroviejo et al., 2011), and other complication factors such as poor exposure, thick soil cover, or poorly understood stratigraphic relationships. The work presented herein provides an approach that may be useful for more effective exploration for VMS deposits in imbricated terranes worldwide. The results illustrate the importance of multi-faceted approach (structural, stratigraphic and chemostratigraphy) to formulate tectono-stratigraphic reconstructions. This approach can help to identify disparate sulphide lenses (e.g., Northwest vs. Main zones), from continuous lenses offset by faults – critical for both exploration and mine planning. Furthermore, fault reconstruction illustrates that while many blocks were lithologically similar (e.g., sequences 1 and 2 vs. sequence 3), they can have distinct structural positions, and may have markedly different economic potential. Consequently, reconstruction of poly-deformed deposits such as presented herein are not only critical to understand the genesis of ancient deposits and their tectonic setting, but also for guiding exploration in deposit-proximal areas. The potential of the later can be further enhanced by the addition of other information layer (e.g.: geochemistry, geophysics, hyperspectral reflectance) within a known geological context, which is key to efficient exploration.

7. Conclusions

The Lemarchant area is underlain by four volcano-sedimentary sequences, one mineralised sequence, and several intrusive phases. Sequences 1 and 2 consist of andesitic breccias, lapilli-tuff and tuff and represent vent-distal volcanoclastic sequences relative to the depositional centre. Sequence 3 consists of vent-proximal andesitic to dacitic autoclastic volcanoclastic and associated massive flows that host the VMS mineralisation. The mineralisation sequence includes exhalative mudstones, massive barite, massive to semi-massive sulphides, chaotic chlorite-carbonate alteration, chlorite alteration and sericite alteration and is principally hosted within the dacitic breccias and flows of sequence 3, with the exception of the exhalative mudstones, which overlay the rocks of sequence 3. Sequence 4 consists of tholeiitic basalts that were deposited conformably on rocks of sequence 3 or on the exhalative mudstone of sequence 3. These sequences are intruded by younger, possibly syn-sequence 4, felsic, intermediate and mafic dikes.

The Lemarchant deposit consists of two distinct VMS lenses that formed within massive dacitic flows and related autoclastic volcanoclastic rocks of sequence 3 that have recorded different deformation styles. The Northwest Zone is hosted in the immediate footwall of the folded LJ syn-volcanic shear zone, whereas the Main Zone occurs in the relatively undeformed hanging wall of the Lemarchant thrust. It is proposed that the tectono-stratigraphic environment of formation of the Lemarchant deposit is within a shallow (<1500 m below sea level) arc or migrating cross-arc seamount chain which produced abundant amount of andesitic rocks. The VMS mineralisation occurs within late dacitic flows (513–509 Ma) that formed during the transition between arc dominated and rift dominated environment. The shallow position of the deposit promoted boiling near or at the seafloor, ultimately resulting in precious metals enrichment of the Lemarchant deposit. It is suggested that arcs or cross-arcs within rifted arc environment represent favourable exploration targets for precious metal enriched VMS deposits.

Deformation of the Lemarchant deposit likely occurred during the Penobscot orogeny (486–478 Ma) and coincided with the deformation of the LJ and KJ syn-volcanic shear zone and subsequent creation of the Lemarchant thrust during a NW-SE compression episode. The late (<465 Ma) east trending Bam normal fault affected the central portion of the Lemarchant area and lowered

the southern portion relative to the northern portion of the studied area.

This study of the Lemarchant deposit resulted in the reconstruction of the original volcanic and structural environment, and has implications for ongoing exploration at Lemarchant and can be used as a framework for other datasets (e.g., geochemistry, geophysics, hyperspectral). The approaches and results presented in this paper are relevant to and can be utilised for understanding and exploring for VMS mineralisation in the Tally Pond group and in similar accretionary orogens globally.

Acknowledgements

Financial support for this project was provided from a Natural Sciences and Engineering Research Council of Canada (NSERC) Collaborative Research and Development Grant to S.J. Piercey. Additional funding was provided by the NSERC-Altius Industrial Research Chair in Mineral Deposits (supported by NSERC, Altius Resources Inc., and the Research and Development Corporation of Newfoundland and Labrador) and an NSERC Discovery Grant to S. J. Piercey. Logistical support was provided by Canadian Zinc Corporation. Diane Fost and Alexandria Marcotte are thank for their incredible support during the field campaigns. Jim Walker and John Hinchey are thanked for their constructive criticism and reviews of the manuscript.

References

- Allen, R.L., 1988. False pyroclastic textures in altered silicic lavas, with implications for volcanic-associated mineralization. *Econ. Geol.* 83, 1424–1446.
- Allen, R.L., Ludström, L., Ripa, M., Simeonov, A., Christofferson, H., 1996. Facies analysis of a 1.9 Ga, continental margin, back-arc, felsic caldera province with diverse Zn-Pb-Ag-(Cu-Au) sulphide and Fe oxide deposits, Bergslagen region, Sweden. *Econ. Geol.* 91, 979–1008.
- Arculus, R.J., 1994. Aspects of magma genesis in arcs. *Lithos* 33, 189–208.
- Calon, T.J., Green, F.K., 1987. Preliminary results of a detailed structural analysis of the Buchans Mine area. *Pap. – Geol. Surv. Can.* 86–24, 273–288.
- Castroviejo, R., Quesada, C., Soler, M., 2011. Post-depositional tectonic modification of VMS deposits in Iberia and its economic significance. *Miner. Deposita* 46, 615–637.
- Cocks, L.R.M., Torsvik, T.H., 2002. Earth geography from 500 to 400 million years ago; a faunal and palaeomagnetic review. *Journal of the Geological Society of London*, v. 159. *J. Geol. Soc. London* 159 (Part 6), 631–644.
- Colman-Sadd, S.P., 1985. Geology of the Burnt Hill Map Area (2D/5), Newfoundland. Mineral Development Division, Department of Mines and Energy, Government of Newfoundland and Labrador, Report 85–3, 94 p., scale 1:50,000.
- Colman-Sadd, S.P., Dunning, G.R., Dec, T., 1992. Dunnage-Gander relationships and Ordovician orogeny in central Newfoundland; a sediment provenance and U/Pb age study. *Am. J. Sci.* 292 (5), 317–355.
- Copeland, D., 2008. The South Tally Pond project: a high-grade polymetallic VMS discovery. *Atlantic Geol.* 45, 55.
- Dunning, G.R., Krogh, T.E., 1985. Geochronology of ophiolites of the Newfoundland Appalachians. *Can. J. Earth Sci.* 22, 1659–1670.
- Dunning, G.R., Swinden, H.S., Kean, B.F., Evans, D.T.W., Jenner, G.A., 1991. A Cambrian island arc in lapetus: geochronology and geochemistry of the Lake Ambrose Volcanic Belt, Newfoundland Appalachians. *Geol. Mag.* 128, 1–17.
- Dunning, G.R., Kean, B.F., Thurlow, J.G., Swinden, H.S., 1987. Geochronology of the Buchans, Roberts Arm, and Victoria Lake Groups and Mansfield Cove complex, Newfoundland. *Can. J. Earth Sci.* 24 (6), 1175–1184.
- Evans, D.T.W., Kean, B.F., 2002. The Victoria Lake supergroup, central Newfoundland – its definition, setting and volcanogenic massive sulphide mineralization. Newfoundland and Labrador Department of Mines and Energy, Geological Survey, Open File NFD/2790. 68 p.
- Evans, D.T.W., Kean, B.F., Dunning, G.R., 1990. Geological studies, Victoria Lake Group, central Newfoundland. Government of Newfoundland and Labrador Department of Mines and Energy, Geological Survey, Report 90-1, pp. 131–144.
- Fisher, R.V., 1966. Rocks composed of volcanic fragments and their classification. *Earth-Sci. Rev.* 1, 287–298.
- Franklin, J.M., Gibson, H.L., Galley, A.G., Jonasson, I.R., 2005. Volcanogenic massive sulfide deposits. In: Hedenquist, J.W., Thompson, J.F.H., Goldfarb, R.J., Richards, J.P. (Eds.), *Economic Geology 100th Anniversary Volume. Society of Economic Geologists*, pp. 523–560.
- Franklin, J.M., Lydon, J.W., Sangster, D.F., 1981. Volcanic-associated massive sulfide deposits. In: Skinner, B.J. (Ed.), *75th Anniversary Volume of Economic Geology*. Lancaster, pp. 485–627.
- Fraser, D., Giroux, G.H., Copeland, D.A., Devine, C.A., 2012. Technical Report and Resource Minerals Estimate on the Lemarchant Deposit, South Tally Pond VMS

- Project, Central Newfoundland, Canada. Paragon Mineral Corporation, Technical Report NI43–101, 132 p.
- Galley, A.G., Hannington, M.D., Jonasson, I.R., 2007. Volcanogenic massive sulphide deposits. In: Goodfellow, W.D. (Ed.), *Mineral Deposits of Canada: A Synthesis of Major Deposit-Types, District Metallogeny, the Evolution of Geological Provinces, and Exploration Methods*. Geological Association of Canada, Mineral Deposits Division, pp. 141–161. Special Publication No. 5.
- Gibson, H.L., Morton, R.L., Hudak, G.J., 1999. Submarine volcanic processes, deposits, and environments favorable for the location of volcanic-associated massive sulphide deposits. In: Barrie, C.T., Hannington, M.D. (Eds.), *Volcanic-associated massive sulphide deposits: Progress and examples in modern and ancient settings*. Reviews in economic geology 8, p. 13–51.
- Gill, S.B., 2015. Mineralogy, metal zoning, and genesis of the Zn-Pb-Ba-Ag-Au Lemarchant volcanogenic massive sulphide (VMS) deposit Unpublished M. Sc. thesis. St. John's, Newfoundland, Memorial University of Newfoundland, p. 167.
- Gill, S.B., Piercy, S.J., 2014. Preliminary mineralogy of barite-associated sulphide mineralization in the Ordovician Zn-Pb-Cu-Ag-Au Lemarchant volcanogenic massive sulphide deposit, Newfoundland and Labrador. *Current Research – Geological Survey of Canada*, p. 15. 2013–17.
- Gill, S.B., Piercy, S.J., Layton-Matthews, D., in press. Mineralogy and metal zoning of the Lemarchant Zn-Pb-Cu-Ag-Au volcanogenic massive sulfide (VMS) deposit, Newfoundland. *The Canadian Mineralogist*.
- Gill, S.B., Piercy, S.J., Layton-Matthews, D., Layne, G.D., Piercy, G., 2015. Mineralogical, sulphur, and lead isotopic study of the Lemarchant Zn-Pb-Cu-Ag-Au-VMS deposit: implications for precious-metal enrichment processes in the VMS environment. In: Peter, J.M., Mercier-Langevin, P. (Eds.), *Targeted Geoscience Initiative 4: Contributions to the Understanding of Volcanogenic Massive Sulphide Deposit Genesis and Exploration Methods Development*; Geological Survey of Canada, Open File 7853, pp. 183–195.
- Gill, S.B., Piercy, S.J., Devine, C.A., 2013. Preliminary mineralogy of barite-associated sulphide mineralization in the Ordovician Zn-Pb-Cu-Ag-Au Lemarchant volcanogenic massive sulphide deposit, Newfoundland and Labrador. *Geological Survey of Canada, Current Research, Report 2013–17*, 15 p.
- Hannington, M.D., 2014. Volcanogenic massive sulfide deposits. In: Holland, H.D., Turekian, K.K. (Eds.), *Treatise on Geochemistry*. second ed. Elsevier, Oxford, pp. 463–488.
- Hawkesworth, C.J., Gallagher, K., Hergt, J.M., McDermott, F., 1993. Mantle and slab contributions in arc magmas. *Annu. Rev. Earth Planet. Sci.* 21, 175–204.
- Hart, T.R., Gibson, H.L., Leshner, C.M., 2004. Trace element geochemistry and petrogenesis of felsic volcanic rocks associated with volcanogenic massive Cu–Zn–Pb sulfide deposits. *Econ. Geol.* 99, 1003–1013.
- Hibbard, J., van Stall, C., Rankin, D., Williams H., 2004. Lithotectonic Map of the Appalachian Orogen, Canada-United States of America, Geological Survey of Canada Map 2096A, scale 1:500,000.
- Hinchee, J.G., McNicoll, V., 2016. The Long Lake Group: An update on U-Pb geochronological studies. *Newfoundland Geological Survey Current Research, Report 16-1*, pp. 27–38.
- Hinchee, J.G., McNicoll, V., 2009. Tectonostratigraphic architecture and VMS mineralization of the southern Tullks volcanic belt: New insights from U-Pb geochronology and lithochemistry. *Newfoundland Geological Survey Current Research, Report 09-1*, pp. 13–42.
- Ishikawa, Y., Sawaguchi, T., Ywaya, S., Horiuchi, M., 1976. Delineation of prospecting targets for Kuroko deposits based on modes of volcanism of underlying dacite and alteration halos. *Min. Geol.* 26, 105–117.
- Jenner, G.A., Swinden, H.S., 1993. The Pipestone Pond complex, central Newfoundland; complex magmatism in an eastern Dunnage zone ophiolite. *Can. J. Earth Sci.* 30 (3), 434–448.
- Johnson, S.C., McLeod, M.J., Fyffe L.R., Dunning, G.R., 2009. Stratigraphy, geochemistry, and geochronology of the Annidae and New River belts, and the development of the Penobscot arc in southern New Brunswick. In: G.L. Martin (Ed.), *Geological Investigations in New Brunswick for 2008*. New Brunswick Department of Natural Resources, Minerals, Policy, and Planning Division, Mineral Resource Report 2009–2, pp. 141–218.
- Kean, B.F., Evans, D.T.W., 1986. Metallogeny of the Tullks Hill Volcanics, Victoria Lake Group, central Newfoundland. Government of Newfoundland and Labrador, Department of Mines and Energy, Mineral Development Division. Report 86–1, pp. 51–57.
- Kean, B.A., Evans, D.T.W., Jenner, G.A., 1995. Geology and mineralization of the Lushs Bight Group. Newfoundland Department of Natural Resources. Report 95–2, 227 p.
- Large, R.R., 1977. Chemical evolution and zonation of massive sulfide deposits in volcanic terrains. *Econ. Geol.* 72, 549–572.
- Large, R.R., Gemmill, J.B., Paulick, H., Huston, D.L., 2001. The alteration box plot: a simple approach to understanding the relationships between alteration mineralogy and lithochemistry associated with VHMS deposits. *Econ. Geol.* 96, 957–971.
- Lentz, D.R., 1998. Petrogenetic evolution of felsic volcanic sequences associated with Phanerozoic volcanic-hosted massive sulfide systems: the role of extensional geodynamics. *Ore Geol. Rev.* 12, 289–327.
- Leshner, C.M., Goodwin, A.M., Campbell, I.H., Gorton, M.P., 1986. Trace element geochemistry of ore-associated and barren felsic meta-volcanic rocks in the Superior province, Canada. *Can. J. Earth Sci.* 23, 222–237.
- Lizasa, K., Fiske, R.S., Ishizuka, O., Yuasa, M., Hashimoto, J., Ishibashi, J., Naka, J., Horii, Y., Fujiwara, Y., Imai, A., Koyama, S., 1999. A Kuroko-type polymetallic sulphide deposit in a submarine caldera. *Science* 283, 975–977.
- Lode, S., Piercy, S.J., Squires, G.C., 2016. Role of metalliferous mudstones and detrital shales in the localization, genesis, and paleoenvironment of volcanogenic massive sulphide deposits of the Tally Pond volcanic belt, central Newfoundland, Canada. *Can. J. Earth Sci.* 53 (4), 387–425.
- Lode, S., Piercy, S., Devine, C.A., 2015. Geology, mineralogy, and lithochemistry of metalliferous mudstones associated with the Lemarchant volcanogenic massive sulphide deposit, Tally Pond Belt, Central Newfoundland. *Econ. Geol.* 110, 1835–1859.
- Lydon, J.W., 1984. Volcanogenic massive sulphide deposits Part 1: A descriptive model. *Geosci. Can.* 11, 195–202.
- Lydon, J.W., 1988. Volcanogenic massive sulphide deposits Part 2: genetic models. *Geosci. Can.* 15, 43–65.
- MacLachlan, K., O'Brien, B.H., Dunning, G.R., 2001. Redefinition of the Wild Bight Group, Newfoundland; implications for models of island-arc evolution in the Exploits Subzone. *Can. J. Earth Sci.* 38 (6), 889–907.
- MacLachlan, K., Dunning, G.R., 1998b. U-Pb ages and tectonomagmatic relationships of Middle Ordovician volcanic rocks of the Wild Bight Group, Newfoundland Appalachians. *Can. J. Earth Sci.* 35, 998–1017.
- MacLachlan, K., Dunning, G., 1998a. U-Pb ages and tectonomagmatic relationships of early Ordovician low-Ti tholeiites, boninites and related plutonic rocks in central Newfoundland, Canada. *Contrib. Mineral. Petrol.* 133 (3), 235–258.
- MacLean, W.H., 1988. Rare earth element mobility at constant inter-REE ratios in the alteration zone at the Phelps Dodge massive sulphide deposit, Matagami, Quebec. *Miner. Deposita* 23, 231–238.
- Marshall, B., Gilligan, L.B., 1987. An introduction to remobilization: information from ore-body geometry and experimental considerations. *Ore Geol. Rev.* 2, 87–131.
- McClay, K.R., 1995. The geometries and kinematics of inverted fault systems: a review of analogue model studies. In: Buchanan, J.G., Buchanan, P.G. (Eds.), *Basin inversion*. Geological Society Special Publication, vol. 88, p. 97–118.
- McDonough, W.F., Sun, S., 1995. Composition of the earth. *Chem. Geol.* 120, 223–253.
- McKenzie, D., Bickle, M.J., 1988. The volume and composition of melt generated by extension of the lithosphere. *J. Petrol.* 29, 625–679.
- McKenzie, D., O'Nions, R.K., 1991. Partial melt distributions from inversion of rare earth element concentrations. *J. Petrol.* 32, 1021–1091.
- McLennan, S.M., 2001. Relationships between the trace element composition of sedimentary rocks and upper continental crust. *Geochem. Geophys. Geosyst.* 2, 24.
- McNicoll, V., Squires, G., Kerr, A., Moore, P., 2010. The Duck Pond and Boundary Cu–Zn deposits, Newfoundland: new insights into the ages of host rocks and the timing of VHMS mineralization. *Can. J. Earth Sci.* 47, 1481–1506.
- McNicoll, V., Squires, G.C., Kerr, A., Moore, P.J., 2008. Geological and metallogenic implications of U-Pb zircon geochronological data from the Tally Pond area, central Newfoundland. Newfoundland and Labrador Department of Natural Resources, Geological Survey, Current Research, Report 08-1, pp. 173–192.
- McPhie, J., Doyle, M., Allen, R.L., 1993. *Volcanic textures: A Guide to the Interpretation of Textures in Volcanic Rocks*. Hobart, Australia. Centre for Ore Deposit and Exploration Studies, University of Tasmania, p. 198.
- Morris, G.A., Larson, P.B., Hooper, P.R., 2000. 'Subduction style' magmatism in a non-subduction setting: the Colville Igneous Complex, NE Washington State, USA. *J. Petrol.* 41, 43–67.
- Nelson, J., 1997. The quiet counter-revolution: structural control of syngenetic deposits. *Geosci. Can.* 24 (2), 91–98.
- O'Brien, B.H., 1991. Geological development of the Exploits and Notre Dame subzones in the New Bay area (parts of NTS 2E/6 and 2E/11), map area, Notre Dame Bay, Newfoundland. Newfoundland Department of Mines and Energy, Geological Survey Division, Current Research, Report 91-1, pp. 155–166.
- O'Brien, B., Swinden, H.S., Dunning, G.R., Williams, S.H., O'Brien, F.H.C., 1997. A peri-Gondwanan arc-back arc complex in Iapetus; Early-Mid Ordovician evolution of the Exploits Group, Newfoundland. *Am. J. Sci.* 297 (2), 220–272.
- Ohmoto, H., 1996. Formation of volcanogenic massive sulphide deposits: the Kuroko perspective. *Ore Geol. Rev.* 10, 135–177.
- Pearce, J.A., 2008. Geochemical fingerprinting of oceanic basalts with application to ophiolite classification and the search for Archean oceanic crust. *Lithos* 100, 14–48.
- Pearce, J.A., 1996. A user's guide to basalt discrimination diagrams. In: Wyman, D.A. (Ed.), *Trace element geochemistry of volcanic rocks: Applications for massive sulfide exploration*, vol. 12. Geological Association of Canada, pp. 79–113. Short Course Notes.
- Pearce, J.A., Peate, D.W., 1995. Tectonic implications of the composition of volcanic arc magmas. *Annu. Rev. Earth Planet. Sci.* 23, 251–285.
- Pearce, J.A., Harris, N.B.W., Tindle, A.G., 1984. Trace element discrimination diagrams for the tectonic interpretation of granitic rocks. *J. Petrol.* 25, 956–983.
- Piercy, S.J., 2011. The setting, style and role of magmatism in the formation of volcanogenic massive sulphide deposits. *Miner. Deposita* 46, 449–471.
- Piercy, S.J., 2010. An overview of petrochemistry in the regional exploration for volcanogenic massive sulphide (VMS) deposits. *Geochem.: Explor. Environ. Anal.* 10, 1–18.
- Piercy, S.J., 2009. Lithochemistry of volcanic rocks associated with volcanogenic massive sulphide deposits and applications to exploration. In: Cousens, B., Piercy, S.J. (Eds.), *Submarine Volcanism and Mineralization: Modern through Ancient*. Geological Association of Canada. Short Course 29-30 May 2008, Quebec City, Canada, pp. 15–40.
- Piercy, S.J., Squires, G.C., Brace, T.D., 2014. Lithostratigraphic, hydrothermal and tectonic setting of the Boundary volcanogenic massive sulphide deposit,

- Newfoundland Appalachians, Canada: Formation by seafloor replacement in a Cambrian rifted arc. *Econ. Geol.* 109, 661–687.
- Piercey, S.J., Murphy, D.C., Mortensen, J.K., Creaser, R.A., 2004. Mid-paleozoic initiation of the northern cordilleran marginal back-arc basin: geological, geochemical and neodymium isotopic evidence from the oldest mafic magmatic rocks in Yukon-Tanana terrane, Finlayson Lake district, southeast Yukon, Canada. *GSA Bull.* 116, 1087–1106.
- Pollock, J., 2004. Geology and paleotectonic history of the Tally Pond Group, Dunnage zone, Newfoundland Appalachians: An integrated geochemical, geochronological, metallogenic and isotopic study of a Cambrian island arc along the Peri-Gondwanan margin of Iapetus. Unpublished M.Sc. thesis, St. John's, Newfoundland, Memorial University of Newfoundland, 420 p.
- Rogers, N., van Staal, C.R., 2002. Toward a Victorial Lake supergroup: A provisional stratigraphic revision of the Red Indian to Victoria Lakes area, central Newfoundland. *Current Research – Newfoundland, Geological Survey Branch. Report 02-1*, pp. 185–195.
- Rogers, N., van Staal, C.R., McNicoll, V., Pollock, J., Zagorevski, A., Whalen, J., 2006. Neoproterozoic and Cambrian arc magmatism along the eastern margin of the Victorial Lake supergroup: a remnant of Ganderian basement in central Newfoundland? *Precamb. Res.* 147, 320–341.
- Ross, P.-S., Bedard, J.H., 2009. Magmatic affinity of modern and ancient subalkaline volcanic rocks determined from trace-element discriminant diagrams. *Can. J. Earth Sci.* 46, 823–839.
- Rudnick, R.L., Fountain, D.M., 1995. Nature and composition of the continental crust – a lower crustal perspective. *Rev. Geophys.* 33, 267–309.
- Ruks, T.W., Piercey, S.J., Ryan, J.J., Villeneuve, M.E., Creaser, R.A., 2006. Mid- to late Paleozoic K-feldspar augen granitoids of the Yukon-Tanana terrane, Yukon, Canada: implications for crustal growth and tectonic evolution of the northern Cordillera. *Geol. Soc. Am. Bull.* 118, 1212–1231.
- Servais, J.W., 1982. Ti-V plots and the petrogenesis of modern and ophiolitic lavas. *Earth Planet. Sci. Lett.* 59, 101–118.
- Spitz, G., Darling, R., 1978. Major and minor element lithogeochemical anomalies surrounding the Louvem copper deposit, Val d'Or, Quebec. *Can. J. Earth Sci.* 15, 1161–1169. <http://dx.doi.org/10.1139/e78-122>.
- Squires, G.C., Hinchey, J.G., 2006. Geology of the Tally Pond volcanic belt and adjacent areas (parts of NTS 12A/09 & 12A/10). Government of Newfoundland and Labrador, Department of Natural Resources, Geological Survey, Map 2006-01, Open File 012A/1202.
- Squires, G.C., Moore, P.J., 2004. Volcanogenic massive sulphide environments of the Tally Pond Volcanics and adjacent area: Geological, lithogeochemical and geochronological results. Newfoundland Department of Mines and Energy, Geological Survey, Current Research. Report 04-1, p. 63-91.
- Squires, G.C., Brace, T.D., Hussey, A.M., 2001. Newfoundland's polymetallic Duck Pond deposit: Earliest Iapetan VMS mineralization formed within a sub-seafloor, carbonate-rich alteration system. In: Evans, D.T.W., Kerr, A. (Eds.), *Geology and Mineral Deposits of the Northern Dunnage Zone, Newfoundland Appalachians*. Geological Association of Canada/Mineralogical Association of Canada, pp. 167–187. Field Trip Guide A2.
- Squires, G.C., MacKenzie, A.C., MacInnis, D., 1991. Geology and genesis of the Duck Pond volcanogenic massive sulphide deposit. In: Swinden, H.S., Evans, D.T.W., Kean, B.F. (Eds.), *Metallogenic framework of base and precious metal deposits, central and western Newfoundland*. Geological Survey of Canada, Open File 2156, pp. 56–64.
- Sun, S.-S., McDonough, W.F., 1989. Chemical and isotopic systematics of oceanic basalts: implications for mantle composition and processes. *Geol. Soc. London*, 313–345. Special Publication 42.
- Swinden, H.S., 1991. Paleotectonic settings of volcanogenic massive sulphide deposits in the Dunnage Zone, Newfoundland Appalachians. *Can. Inst. Min. Metall. Bull.* 84, 59–89.
- Swinden, H.S., Jenner, G.A., Kean, B.F., Evans, D.T.W., 1989. Volcanic rock geochemistry as a guide for massive sulphide exploration in central Newfoundland. Government of Newfoundland and Labrador, Department of Mines and Energy, Mineral Development Division (St. John's, 1985), Report of Activities 89–1, pp. 201–209.
- Swinden, H.S., 1996. The application of volcanic geochemistry in the metallogeny of volcanic-hosted sulphide deposits in central Newfoundland. In: Wyman, D.A. (Ed.), *Trace element geochemistry of volcanic rocks: Applications for massive sulfide exploration*, vol. 12. Geological Association of Canada, pp. 329–358. Short Course Notes.
- Tatsumi, Y., Eggins, S., 1995. Subduction Zone Magmatism. Blackwell, Cambridge.
- Thurlow, J.G., 1996. Geology of a newly discovered cluster of blind massive-sulphide deposits, Pilley's Island, central Newfoundland. In: Pereira, C.P.G., Walsh, D.G. (Eds.), *Current Research Report, Report: 96–1*. Geological Survey of Newfoundland and Labrador, St. John's, NL, pp. 181–189.
- van Staal, C.R., 1994. The Brunswick subduction complex in the Canadian Appalachians: record of the Late Ordovician to Late Silurian collision between Laurentia and the Gander margin of Avalon. *Tectonics* 13, 946–962.
- van Staal, C.R., 2007. Pre-Carboniferous metallogeny of the Canadian Appalachians. In Goodfellow, W.D. (Ed.), *Mineral Deposits of Canada: A Synthesis of Major Deposit Types, District Metallogeny, the Evolution of Geological Provinces, and Exploration Methods*. Mineral Deposits Division, Geological Association of Canada, Special Publication 5, pp. 793–818.
- van Staal, C.R., Barr, S.M., 2012. Lithospheric architecture and tectonic evolution of the Canadian Appalachians and associated Atlantic margin. Chapter 2 in Percival, J.A., Cook, F.A., Clowes, R.M. (Eds.), *Tectonic Styles in Canada: the LITHOPROBE Perspective*. Geological Association of Canada, Special Paper 49, pp. 41–96.
- van Staal, C.R., Colman-Sadd, S.P., 1997. The central Mobile Belt of the Northern Appalachians. *Oxford Monogr. Geol. Geophys.* 35, 747–760.
- Vivallo, W., and Claesson, L.-A., 1987. Intra-arc rifting and massive sulphide mineralization in an early Proterozoic volcanic arc, Skellefte district, northern Sweden. In: Pharaoh, T.C., Beckinsale, R.D., Rickard, D. (Eds.), *Geochemistry and Mineralization of Proterozoic Volcanic Suites*, Geological Society Special Publication No. 33, pp. 69–79.
- White, J.D.L., Houghton, B.F., 2006. Primary volcanoclastic rocks. *Geology* 34 (8), 677–680.
- William-Jones, A.E., Bowell, R.J., Migdisov, A.A., 2009. Gold in solution. *Elements* 5, 281–287.
- Williams, H., 1979. Appalachian Orogen in Canada. *Can. J. Earth Sci.* 21, 887–901.
- Williams, H., Colman-Sadd, S.P., Swinden, H.S., 1988. Tectonostratigraphic subdivisions of central Newfoundland. In *Current Research, Part B. Geological Survey of Canada, Paper 88–1B*, pp. 91–98.
- Winchester, J.A., Floyd, P.A., 1977. Geochemical discrimination of different magma series and their differentiation products using immobile elements. *Chem. Geol.* 20, 325–343.
- Wright, I.C., Parson, L.M., Gamble, J.A., 1996. Evolution and interaction of migrating cross-arc volcanism and backarc rifting: an example from the southern Havre Trough (35°20'–37°S). *J. Geophys. Res.* 101 (B10), 22071–22086.
- Zagorevski, A., van Staal, C.R., Rogers, N., McNicoll, V., Dunning, G.R. and Pollock, J. C., 2010. Middle Cambrian to Ordovician arc-backarc development on the leading edge of Ganderia, Newfoundland Appalachians. In *From Rodinia to Pangea: The Lithotectonic Record of the Appalachian Region*. Edited by R.P. Tollo, M.J. Batholomew, J.P. Hibbard, and P.M. Karabinos. Geological Society of America, Memoir 206, pp. 367–396.
- Zagorevski, A., van Staal, C.R., McNicoll, V., Rogers, N., Valverde-Vaquero, P., 2008. Tectonic architecture of an arc-arc collision zone, Newfoundland Appalachians. In: Draut, A., Clift, P.D., and Scholl, D.W. (Eds.), *Formation and Applications of the Sedimentary Record in Arc Collision Zones*. Geological Society of America, Special Paper 436, pp. 309–334.
- Zagorevski, A., van Staal, C.R., McNicoll, V.J., Rogers, N., 2007. Upper Cambrian to Upper Ordovician peri-Gondwanan island arc activity in the Victorial Lake supergroup, central Newfoundland: tectonic development of the northern Ganderian margin. *Am. J. Sci.* 307, 339–370.
- Zagorevski, A., van Staal, C.R., McNicoll, V.J., 2007. Distinct Taconic, Salinic, and Acadian deformation along the Iapetus suture zone, Newfoundland Appalachians. *Can. J. Earth Sci.* 44, 1567–1585.
- Zagorevski, A., Rogers, N., McNicoll, V., Lissenberg, C.J., van Staal, C.R., Valverde-Vaquero, P., 2006. Lower to Middle Ordovician evolution of peri-Laurentian arc to back-arc complexes in the Iapetus: constraints from the Annieopsquotch accretionary tract, central Newfoundland. *Geol. Soc. Am. Bull.* 118 (3/4), 324–342.